

Sensitivity of photolysis frequencies and key tropospheric oxidants in a global model to cloud vertical distributions and optical properties

Hongyu Liu¹, James H. Crawford², David B. Considine², Steven Platnick³, Peter M. Norris^{3,4}, Bryan N. Duncan^{3,4}, Robert B. Pierce^{2,5}, Gao Chen², and Robert M. Yantosca⁶

¹National Institute of Aerospace, Hampton, VA

²NASA Langley Research Center, Hampton, VA

³NASA Goddard Space Flight Center, Greenbelt, MD

⁴University of Maryland, Baltimore County, MD

⁵Now at NOAA/NESDIS/STAR, WI

⁶Harvard University, Cambridge, MA

Short Title: Sensitivity of Photochemistry to Clouds

Keywords: photolysis rate, tropospheric ozone, hydroxyl radical, solar radiation, cloud optical depth, cloud absorption, cloud overlap, 3-D global CTM

Journal of Geophysical Research-Atmospheres; in press, March 2009

Correspondence: Hongyu Liu
Mail Stop 401B, NASA Langley Research Center
Hampton, VA 23681
Tel: 757-864-3191; Fax: 757-864-6326
Email: [hyl \(at\) nianet.org](mailto:hyl(at)nianet.org)

Abstract. Clouds directly affect tropospheric photochemistry through modification of solar radiation that determines photolysis frequencies. As a follow-up study to our recent assessment of these direct radiative effects of clouds on tropospheric chemistry, this paper presents an analysis of the sensitivity of such effects to cloud vertical distributions and optical properties (cloud optical depths (CODs) and cloud single scattering albedo), in a global 3-D chemical transport model (GEOS-Chem). GEOS-Chem was driven with a series of meteorological archives (GEOS1-STRAT, GEOS-3 and GEOS-4) generated by the NASA Goddard Earth Observing System data assimilation system. Clouds in GEOS1-STRAT and GEOS-3 have more similar vertical distributions (with substantially smaller CODs in GEOS1-STRAT) while those in GEOS-4 are optically much thinner in the tropical upper troposphere. We find that the radiative impact of clouds on global photolysis frequencies and hydroxyl radical (OH) is more sensitive to the vertical distribution of clouds than to the magnitude of column CODs. With random vertical overlap for clouds, the model calculated changes in global mean OH ($J(\text{O}^1\text{D})$, $J(\text{NO}_2)$) due to the radiative effects of clouds in June are about 0.0% (0.4%, 0.9%), 0.8% (1.7%, 3.1%), and 7.3% (4.1%, 6.0%), for GEOS1-STRAT, GEOS-3 and GEOS-4, respectively; the geographic distributions of these quantities show much larger changes, with maximum decrease in OH concentrations of ~15-35% near the midlatitude surface. The much larger global impact of clouds in GEOS-4 reflects the fact that more solar radiation is able to penetrate through the optically thin upper-tropospheric clouds, increasing backscattering from low-level clouds. Model simulations with each of the three cloud distributions all show that the change in the global burden of ozone due to clouds is less than 5%. Model perturbation experiments with GEOS-3, where the magnitude of 3-D CODs are progressively varied from -100% to 100%, predict only modest changes (<5%) in global mean OH concentrations. $J(\text{O}^1\text{D})$, $J(\text{NO}_2)$ and OH concentrations show the strongest sensitivity for small CODs and become insensitive at large CODs due to saturation effects. Caution should be exercised not to use in photochemical models a value for cloud single scattering albedo lower than about 0.999 in order to be consistent with the current knowledge of cloud absorption at the ultraviolet wavelengths.

1. Introduction

Tropospheric ozone (O_3) is an important greenhouse gas, and hydroxyl radical (OH) determines the oxidative capacity of the troposphere [Thompson, 1992]. Any perturbations to O_3 and OH have important implications for climate change [IPCC, 2001]. Clouds directly affect tropospheric photochemistry through modification of solar radiation that determines photolysis frequencies [Thompson *et al.*, 1984; Madronich, 1987; Crawford *et al.*, 1999], in addition to their roles in tropospheric chemistry via the processes of heterogeneous chemistry, wet removal, convective transport of trace gases and aerosols, and nitrogen oxides (NO_x) emissions due to lightning associated with deep convective clouds. However, there have been few studies of the impact of clouds on photolysis frequencies and tropospheric oxidants such as O_3 and OH on a global scale [Krol and van Weele, 1997; Tie *et al.*, 2003; Liu *et al.*, 2006]. Cloud amounts and distributions may very well change in a changing climate and better understanding of the global impact of clouds is essential for predicting the feedback of climate change on tropospheric chemistry. We recently assessed the radiative effects of clouds on photolysis frequencies and key oxidants in the troposphere with GEOS-Chem [Liu *et al.*, 2006], a global three-dimensional (3-D) chemical transport model (CTM) driven by assimilated meteorological observations. In this paper, we apply the same model to examine the sensitivity of this effect to the uncertainty associated with the distributions and optical properties of clouds.

Modeling studies of the radiative effects of clouds on tropospheric chemistry have emphasized the need to account for the spatial and temporal variability of photolysis frequencies under different atmospheric (including cloud) conditions [Wild *et al.*, 2000; Mao *et al.*, 2003; Tang *et al.*, 2003; Tie *et al.*, 2003; Yang and Levy, 2004; Liu *et al.*, 2006]. Results indicated that photolysis frequencies are enhanced above and in the upper portion of cloud layers and are reduced below optically thick clouds, consistent with observations [Lefer *et al.*, 2003]. Including in the model the effect of vertical subgrid variability of cloudiness (cloud overlap) on radiative transfer has a significant impact on above-cloud (below-cloud) enhancements (reductions) [Feng *et al.*, 2004; Liu *et al.*, 2006]. Nevertheless, we found that regardless of the different assumptions about cloud overlap, the global average effect remained modest in GEOS-Chem when the model was driven by the GEOS-3 assimilated meteorology, reflecting an offsetting effect above and below clouds [Liu *et al.*, 2006]. This was consistent with the finding of Krol and Weele [1997] who found that the effect of clouds on the globally averaged lifetime of methane (CH₄) was small due to compensating effects above and below clouds.

Previous estimates of the radiative impact of clouds on global tropospheric chemistry were based on CTMs driven by different meteorology that contained different cloud fields, either from general circulation models (GCMs) [e.g., Tie *et al.*, 2003; Wu *et al.*, 2007] or from data assimilation systems [e.g., Liu *et al.*, 2006; Wu *et al.*, 2007]. The representation of clouds in current climate models is still a challenging task because cloud processes typically take place on scales that are not adequately resolved by these models and have to be parameterized [Quante, 2004; Stephens, 2005]. Recently, Zhang *et al.* [2005] compared clouds in ten GCMs and found that the majority of the models overestimated optically thick clouds by over a factor of 2, while underestimating optically intermediate and optically thin clouds. The uncertainty in simulated clouds (and relevant radiative processes) has been recognized as a large limiting factor in current assessments of climate change [IPCC, 2001, 2007].

As a follow-up study to our recent assessment of the radiative effects of clouds on tropospheric chemistry [Liu *et al.*, 2006], this paper presents an analysis of the sensitivity of this effect to cloud vertical distributions and optical properties with the use of GEOS-Chem [Bey *et al.*, 2001; Park *et al.*, 2004] coupled with the Fast-J radiative transfer model [Wild *et al.*, 2000]. We drive GEOS-Chem with a series of meteorological archives from the Goddard Earth Observing System data assimilation system (GEOS DAS) at the NASA Global Modeling and Assimilation Office (GMAO), which are characterized by distinctly different cloud fields, in particular cloud vertical distributions and CODs. We will show that the radiative impact of clouds on global tropospheric chemistry is more sensitive to the vertical distribution of clouds than to the magnitude of CODs, and is also sensitive to the assumption about cloud absorption. We will also show that differing optical depths and vertical distributions of clouds cannot explain the contrasting sensitivities of tropospheric photochemistry to clouds in the two modeling studies of Tie *et al.* [2003] and Liu *et al.* [2006].

The paper is organized as follows. Section 2 gives a brief description of the GEOS-Chem model and its evaluation with observations. Section 3 presents the cloud fields in three GEOS meteorological archives and their evaluations with satellite observations. The sensitivities of photolysis frequencies and key oxidants to cloud vertical distributions, CODs, and cloud absorption of solar radiation are examined in sections 4 through 7, followed by summary and conclusions in section 8.

2. Model Description

GEOS-Chem is a global 3-D model of tropospheric O₃-NO_x-hydrocarbon chemistry coupled to aerosol chemistry, driven by assimilated meteorological observations with 3- to 6-hour resolution from the Goddard Earth Observing System (GEOS) of the NASA Global Modeling and Assimilation Office (GMAO). It solves the chemical evolution of ~90 species and transports 41 chemical tracers. The initial description of the model as applied to simulation of tropospheric O₃-NO_x-hydrocarbon chemistry was presented by *Bey et al.* [2001], with significant updates by *Martin et al.* [2002], *Park et al.* [2004] and *Evans and Jacob* [2005]. In particular, *Park et al.* [2004] coupled aerosol (including sulfate-nitrate-ammonium, carbonaceous aerosols, sea salt, and mineral dust) chemistry with O₃-NO_x-hydrocarbon chemistry. The model simulation of global tropospheric chemistry using different generations of GEOS assimilated meteorology has been evaluated in a number of studies since it was first evaluated by *Bey et al.* [2001]. The reader is referred to *Liu et al.* [2006] for a brief review. In this study we use GEOS-Chem version 7.1 (see <http://www.as.harvard.edu/ctm/geos/>) [*Heald et al.*, 2006; *Martin et al.*, 2006]. Global simulations of tropospheric chemistry were conducted for the years of 1996 and 2001. The simulation years were chosen so as to use different meteorological archives that have different cloud fields. All simulations in this study were conducted with five-month initialization and we analyze the model results for the years of 1996 and 2001.

Three generations of GEOS meteorological products are used for the simulation years as follows: GEOS1-STRAT for 1996 (2° latitude × 2.5° longitude horizontal resolution, 46 vertical levels, top at 0.1 hPa), GEOS-3 (1° latitude × 1° longitude, 48 levels, top at 0.01 hPa) and GEOS-4 both for 2001 (1° latitude × 1.25° longitude, 55 levels, top at 0.01 hPa, *Bloom et al.* [2005]). We have not included the latest GEOS-5 meteorological product because our main focus is on the sensitivity of tropospheric chemistry to different aspects (column integral and vertical distribution) of the COD. The three archives used (GEOS1-STRAT, GEOS-3 and GEOS-4) provide continuity with our previous paper [*Liu et al.*, 2006] and provide enough variability in the COD distributions for the current sensitivity study. For computational expediency, we degrade the horizontal resolution to 4°×5° and merge the 23 (26, 36) vertical levels above 50 (85, 80) hPa for GEOS1-STRAT (GEOS-3, GEOS-4), retaining a total of 26 (30, 30) vertical levels. The vertical levels for GEOS1-STRAT and GEOS-3 are defined along a sigma coordinate. GEOS-4 employs a hybrid sigma-pressure coordinate system; the lowest 14 levels are pure sigma levels and the rest (mainly above 200hPa) fixed pressure levels. The midpoints of the lowest four levels in the GEOS1-STRAT (GEOS-4) data are at 50 (60), 250 (250), 600 (610), and 1100 (1200) m above the surface for a column based at sea level. The GEOS-3 data have finer resolution of the boundary layer with layer midpoints at 10, 50, 100, 200, 350, 600, 850, and 1250m above the surface. The cross-tropopause flux of O₃ is specified with the Synoz (synthetic O₃) scheme [*McLinden et al.*, 2000] by imposing a global net cross-tropopause flux of 475 Tg O₃ per year (GEOS1-STRAT), 500 Tg O₃ per year (GEOS-3), and 495 Tg O₃ per year (GEOS-4); the variability partly reflects the difference in circulations between meteorological archives. A uniform global CH₄ concentration of 1700 ppbv is imposed.

Photolysis frequencies are calculated with the Fast-J radiative transfer algorithm of *Wild et al.* [2000], which uses a seven-wavelength quadrature scheme and accounts accurately for Rayleigh scattering as well as Mie scattering by aerosols and clouds. A total of 52 photolysis reactions are included and photolysis calculations are performed every hour. Vertically resolved CODs and cloud fractions are taken from the GEOS meteorological archives with 6-hour resolution. To take into account cloud overlap, we use in this paper the Approximate Random

Overlap (RAN) scheme unless explicitly stated. The RAN scheme assumes that the grid average COD is

$$\tau_c' = \tau_c f^{3/2} \quad (1)$$

where τ_c is the COD in the cloudy portion of the grid and f is the cloud fraction in each layer [Briegleb, 1992]. The column COD is the sum of τ_c' for each layer of the column. Briegleb [1992] showed that RAN yields a reasonable approximation to a detailed random overlap calculation for the heating rate. RAN is also a good approximation of the maximum-random overlap, which is more computationally expensive, in terms of the radiative impact of clouds on tropospheric chemistry (see discussions in Liu *et al.* [2006]). Because the linear scheme (LIN), where $\tau_c' = \tau_c f$, was used for standard tropospheric chemistry simulations in all previous papers using GEOS-Chem, we also present model results with LIN when quantifying the global mean radiative effects of clouds (**Table 1**) for comparison purposes. Clouds are assumed to be fully scattering (i.e., cloud single scattering albedo SSA=1.0). Monthly mean surface albedos are those of Herman and Celarier (1997). The model uses climatological O₃ concentrations as a function of latitude, altitude, and month to calculate the absorption of UV radiation by O₃. Using tropospheric O₃ concentrations from the model simulation (vs. climatology) has little effect on our results [Liu *et al.*, 2006].

The radiative effects of clouds in the model are represented by subtraction of a clear-sky simulation from a cloudy-sky simulation. In the clear-sky simulation CODs are set to zero in the calculation of photolysis frequencies while other roles of clouds (i.e., transport, wet removal, heterogeneous chemistry and lightning NO_x emissions associated with deep convective clouds) are present in both the clear-sky and cloudy-sky simulations.

3. Cloud Fields

In this section, we describe briefly how clouds are formed, intercompare CODs in the three GEOS meteorological archives, and evaluate the model diagnosed CODs with global satellite observations. Since Fast-J requires as input the grid-scale COD in vertical model layers, the intercomparison and evaluation will help us understand the sensitivities of tropospheric chemistry to these cloud fields.

3.1. Cloud Formation

In GEOS1-STRAT, convective and large-scale cloudiness are diagnosed as part of the cumulus and large-scale parameterizations [Takacs *et al.*, 1994]. They are combined into random overlap (CLRO) and maximum overlap (CLMO) cloudiness. The total cloud fraction, f , at each level is then obtained by: $f = 1 - (1-CLRO) \cdot (1-CLMO)$. CODs are specified based on cloud type and temperature. The “maximum overlap” clouds are assigned an optical depth of 16 per 100mb and the “random overlap” clouds are assigned an optical depth based on an empirical relation between local temperature and optical depth.

In GEOS-3, the occurrence of clouds is empirically diagnosed based on grid-scale relative humidity and subgrid-scale convection. For large-scale clouds, COD is empirically assigned values proportional to the diagnosed large-scale liquid water. For convective clouds, COD is prescribed as 16 per 100mb. A temperature-dependence is used to distinguish between water and ice clouds. The total optical depth in a given model layer is computed as a weighted average between the large-scale and subgrid scale optical depths, normalized by the total cloud fraction in the layer.

In GEOS-4 and its parent general circulation model fvGCM (finite-volume GCM), the physics was adopted from the NCAR CCM3 (Community Climate Model version 3) and

WACCM (Whole Atmosphere Community Climate Model) with several modifications [Kiehl *et al.*, 1998]. The cloud microphysics follows the simple diagnostic condensate parameterization in the standard CCM3. The diagnosis of cloud fraction uses a modified *Slingo* [1987] scheme. Cloud fraction depends on relative humidity, vertical velocity, atmospheric stability and convective mass fluxes. The scheme diagnoses three types of cloud, i.e., low-level marine stratus, convective cloud, and layered cloud. The parameterization of cloud optical properties is described in Kiehl *et al.* [1998].

3.2. Evaluation of GEOS Cloud Optical Depths with Satellite Observations

Since information about the global climatology of the vertical distribution of cloud water/ice content and optical depth is currently lacking, we focus on column CODs when evaluating model cloud fields against the observations. Satellite retrieved products of column CODs are available from the Moderate Resolution Imaging Spectroradiometer (MODIS) [Platnick *et al.*, 2003] and the International Satellite Cloud Climatology Project (ISCCP) [Rossow *et al.*, 1996; Rossow and Schiffer, 1999]. The standard ISCCP D2 data set [Rossow *et al.*, 1996] reports as column CODs the averaged values of individual pixels with nonlinear weights that preserve the average cloud albedo (the so-called “radiative mean CODs” [Rossow *et al.*, 2002]), while storing linear averages of individual pixel values of optical depth (the so-called “linear mean CODs” [Rossow *et al.*, 2002]) in the form of mean cloud water content. It is important to note that ISCCP radiative mean CODs are about a factor of 2-3 smaller than the linear mean CODs (W.B. Rossow, personal communication, 2004). The MODIS data set provides linear mean CODs and geometric mean CODs, the latter being a proxy for radiative mean CODs [e.g., Oreopoulos and Cahalan, 2005].

We previously compared in Liu *et al.* [2006] GEOS-3 monthly (linear mean) CODs with MODIS (MOD08_M3.004) and ISCCP (D2, linear mean) retrievals for the year of 2001. We made a similar comparison between GEOS1-STRAT, GEOS-3, GEOS-4, MODIS (MOD08_M3.005) and ISCCP (D2) datasets for June (not shown). Both MODIS and ISCCP CODs show peaks in the tropics and at mid-latitudes in the Northern Hemisphere (NH) and the marine stratus region in the Southern Hemisphere (SH, ~50-60°S). GEOS CODs show similar features, with GEOS1-STRAT and GEOS-4 CODs substantially lower than the satellite retrievals by factors of about 5 and 2, respectively. The GEOS CODs we used are diurnal averages, but they are almost identical (in a zonal mean sense) to the daytime averages. Although GEOS-3 CODs are closest to the satellite retrievals, GEOS-3 tends to overestimate CODs in the tropics and NH lower mid-latitudes (extending from the subtropics). MODIS and ISCCP retrievals show high CODs at high southern latitudes, presumably due to errors associated with COD retrievals over snow or ice cover. ISCCP seems to have a similar problem in the summer (NH) very high latitudes, though MODIS appears to do much better in this latter case. This comparison, however, did not take into account how clouds overlap in the vertical.

We improve the comparison between GEOS and satellite CODs by considering cloud overlap. MODIS and ISCCP observations of global cloudiness assume only a single cloud layer is present in a given pixel and therefore implicitly include the effects of cloud overlap. Since we use in this study the RAN cloud overlap scheme in our model standard simulation, we compare the GEOS effective column CODs under the RAN scheme with MODIS and ISCCP all-sky grid-box (radiative mean) CODs (**Figure 1a**). GEOS CODs are τ_c' values in equation (1) integrated in the vertical column. MODIS and ISCCP all-sky grid-box CODs are averages over both grid-box cloudy and clear areas with nonlinear weights that preserve the average cloud albedo, as derived in the **Appendix**.

MODIS radiative mean CODs are very close to those of ISCCP in the tropics while the former is somewhat larger at mid-latitudes. As with linear mean CODs (not shown), MODIS and ISCCP radiative mean CODs also show peaks in the tropics and mid-latitudes (**Figure 1a**). Relative to linear mean CODs, GEOS effective CODs under the RAN scheme (**Figure 1a**) have smaller magnitude with similar latitudinal variations. These CODs also differ substantially among the GEOS archives. In the tropics, GEOS-4 effective CODs are most close to MODIS and ISCCP radiative mean CODs; at mid-latitudes, GEOS-4 and GEOS-3 effective CODs appear to bracket MODIS and ISCCP radiative mean CODs.

Figure 1b shows the relevant zonal mean total cloud fractions. The MODIS MOD35 cloud-mask fraction (i.e., “Cloud_Fraction_Mean_Mean” in the Collection 5 processing stream) is very close to the ISCCP cloud fraction. Both are diurnal-mean cloud fractions. Note that the MOD35 *daytime*-mean cloud-mask fraction (not shown) is very close to the corresponding diurnal-mean fraction. This indicates that there is not a large diurnal variation, at least in the zonal means, and justifies the combination of diurnal-mean ISCCP cloud fractions and the daytime-mean ISCCP CODs in the ISCCP all-sky calculations for Figures 1a and 1b. Relative to total cloud fractions in GEOS1-STRAT and GEOS-4, those in GEOS-3 appear to better agree with ISCCP retrievals as well as total cloud fractions from the MOD35 cloud mask. A similar under-prediction of GEOS-4 zonal mean cloud fraction was reported by *Norris and da Silva* [2007] for January 2001.

Also shown in **Figure 1b** (thick solid line) is the MOD06 COD-retrieval cloud fraction (“Cloud_Fraction_Combined_FMean”). This is the fraction of MODIS pixels classified as cloudy for the purposes of doing COD retrievals. This is the appropriate cloud fraction to use for MODIS all-sky COD calculations and the one used in **Figures 1a**. It is significantly smaller than the cloud-mask fraction, because the MODIS COD retrieval algorithms are more selective than the cloud mask in order to return accurate COD values. This increased selectivity tends to remove dubiously cloudy pixels that tend to have very small COD values anyway, so does not produce an underestimate of all-sky COD. This was verified against Collection 004 retrievals (not shown), which were less selective, with higher cloud fractions, but produced all-sky CODs similar to Collection 005 values.

Discrepancies between CODs in the three GEOS archives include not only their magnitudes but vertical distributions. We intercompare in **Figure 2** the latitude-height cross sections of monthly zonal mean effective cloud extinction coefficients (km^{-1}) and cloud fractions in GEOS1-STRAT (1996), GEOS-3 (2001) and GEOS-4 (2001) for June. Clouds in GEOS-4 are optically much thinner in the tropical upper troposphere compared to those in GEOS1-STRAT and GEOS-3; the latter two cases exhibit more similar spatial (especially vertical) cloud extinction distributions, even though the GEOS1-STRAT values are smaller in magnitude.

The global distributions of GEOS1-STRAT, GEOS-3, and GEOS-4 monthly mean column effective CODs are shown in **Figure 3** in comparison with MODIS and ISCCP all-sky grid-box radiative mean CODs for March 2001 when frequent cyclogenesis occurred in the NH. Note the smaller color scale for GEOS1-STRAT. Also shown in **Figure 3** are the probability distribution functions (PDF) of global monthly mean column CODs in each dataset. CODs in all GEOS archives show maxima in the tropics associated with deep convective clouds and at midlatitudes associated with extratropical cyclones in the NH and marine stratiform clouds in the SH. Despite the different magnitudes of column CODs among the three archives, their features in the global distributions (i.e., maxima in the tropics and at midlatitudes) are consistent with those in the MODIS and ISCCP cloud retrieval products. Their probability distribution functions

indicate that CODs in the range of 1-3 are mostly seen in all GEOS archives (except GEOS1-STRAT) as well as MODIS and ISCCP retrievals.

4. Sensitivity of Photolysis Frequencies to Cloud Optical Depths

In this section, we examine the sensitivity of the global impact of GEOS1-STRAT, GEOS-3, and GEOS-4 clouds on photolysis frequencies. We focus on $J(\text{O}^1\text{D})$ and $J(\text{NO}_2)$, which are the most critical parameters for determining OH and O_3 concentrations [Thompson and Stewart, 1991].

Figure 4 shows the simulated percentage changes in the June monthly daily mean $J(\text{O}^1\text{D})$ due to the radiative effects of clouds with GEOS1-STRAT, GEOS-3, and GEOS-4, respectively. With GEOS1-STRAT and GEOS-3, $J(\text{O}^1\text{D})$ in the tropics is enhanced by up to ~10-15% above the high clouds, and reduced by up to ~5-10% (GEOS1-STRAT) and ~10-20% (GEOS-3) below. These enhancements (reductions) reflect the backscattering (attenuation) of solar UV radiation above (below) the deep convective clouds. Similar effects are also seen above and below the low-level clouds at NH and SH midlatitudes. Overall, GEOS1-STRAT and GEOS-3 yield similar patterns in terms of the regions of $J(\text{O}^1\text{D})$ enhancements and reductions due to the radiative impact of clouds, reflecting their similar vertical distributions of clouds (**Figure 2**). However, relative to GEOS1-STRAT, GEOS-3 gives larger enhancements (reductions) above (below) the clouds because of larger CODs.

By contrast, with GEOS-4, $J(\text{O}^1\text{D})$ is enhanced (by ~5-10%) in most of the tropical troposphere and is reduced (by ~5%) only near the surface (<~1km). The optically much thinner clouds in the tropical upper troposphere in GEOS-4 allow more solar UV radiation to penetrate through and be subsequently reflected by low-level thick clouds. The net changes in $J(\text{O}^1\text{D})$ in the tropical middle troposphere are determined by the competition between the radiative effects of high and low clouds. Indeed, the optically thicker clouds in the tropical upper troposphere in GEOS1-STRAT and GEOS-3 allow less solar UV radiation to penetrate down, resulting in net reductions in the middle troposphere.

The sensitivity of $J(\text{NO}_2)$ to the three cloud fields is spatially similar to that of $J(\text{O}^1\text{D})$ but has a larger magnitude (not shown); the latter was discussed in Liu *et al.* [2006].

5. Sensitivity of Key Oxidants to Cloud Optical Depths

We examine in this section the sensitivity of OH and O_3 calculations to the CODs in the three meteorological archives. Model results are discussed in terms of global means (section 5.1) and monthly zonal means (section 5.2).

5.1. Global Mean

Shown in **Table 1** are the simulated percentage changes in the global mean concentrations of key oxidants in the troposphere, photolysis frequencies and global mean lifetimes of methylchloroform (CH_3CCl_3 , MCF) and CH_4 due to the radiative effects of clouds with the GEOS1-STRAT (1996), GEOS-3 (2001), and GEOS-4 (2001) meteorological archives for June and January. Results with both RAN and LIN cloud overlap assumptions are shown; LIN was used in previous standard versions of the GEOS-Chem model and the corresponding results are presented here for comparison. With GEOS1-STRAT, calculated global mean changes in OH, O_3 , NO_x , HO_2 , CH_2O , CO, $J(\text{O}^1\text{D})$, $J(\text{NO}_2)$, and $J(\text{CH}_2\text{O})$ for June are generally less than a few percent, using either RAN or LIN. We found the same (i.e., less than ~6%) previously with GEOS-3 [Liu *et al.*, 2006]. The slight differences between the model results for GEOS-3 reported in **Table 1** here and Table 2 of Liu *et al.* [2006] reflect an updated version of the model

used in this study. In January, both GEOS1-STRAT and GEOS-3 yield global mean changes that are still less than $\sim 6\%$ (RAN) or $\sim 9\%$ (LIN). As we discussed in section 4 and will discuss further below, the global mean effects are similar for these two meteorological archives because of their similar vertical distribution of clouds, even though their column CODs differ by a factor of about 5. The fact that the global mean effect remains modest when driven with GEOS1-STRAT or GEOS-3 reflects mainly an offsetting effect of above-cloud enhancements and below-cloud reductions.

GEOS-4 cloud perturbations to global mean OH concentrations and photolysis frequencies are much larger than occurs with either GEOS1-STRAT or GEOS-3, in particular when LIN is used for cloud overlap. For instance, global mean OH concentrations change by $\sim 7\%$ (RAN) or $\sim 13\%$ (LIN) due to the effects of clouds in GEOS-4 (versus $< \sim 2\%$ change in GEOS1-STRAT and GEOS-3). This is surprising given that the column CODs in GEOS-4 are larger (smaller) than those in GEOS1-STRAT (GEOS-3) by a factor of ~ 2.5 (2). The larger global mean effect in our model with GEOS-4 results from the fact that optically thin upper-tropospheric clouds allow the (optically thick) lower-tropospheric clouds to have a large radiative effect. In other words, solar radiation can penetrate through the upper troposphere and is reflected by low-level thick clouds, increasing photochemical activity in most of the troposphere. Such large effects of clouds on OH were also seen in GEOS-Chem simulations driven by GISS GCM meteorological data, which has thick clouds in the tropical lower troposphere [Wu *et al.*, 2007]. On the other hand, with GEOS-4, the differences in cloud perturbations to global mean OH concentrations and photolysis frequencies due to the RAN and LIN assumptions used in the model are much larger than those with GEOS1-STRAT and GEOS-3. It is because the optically much thinner (thicker) high clouds in GEOS-4 (GEOS1-STRAT and GEOS-3) enhance (reduce) the effect of different assumptions about cloud overlap on the reflection from low clouds.

We calculated the lifetimes of MCF and CH_4 , proxies for the global mean OH concentrations. With GEOS1-STRAT or GEOS-3, the annual mean lifetime of MCF (CH_4) increases by less than a few percent as a result of the radiative effects of clouds (**Table 1**). We find that the MCF (CH_4) lifetime may increase even if global mean OH concentrations increase. This is because the MCF-OH (CH_4 -OH) reaction constant is temperature dependent and the MCF (CH_4) lifetime is more sensitive to the OH concentrations in the lower troposphere (versus the middle and upper troposphere) and the tropics (versus higher latitudes). With GEOS-4, annual mean lifetimes of MCF and CH_4 decrease by 6% (RAN) or 11% (LIN) due to the effects of clouds. As we will show below, this large decrease compared to that with GEOS1-STRAT or GEOS-3 reflects the broader increases in OH concentrations in the free troposphere, including the tropics, in the model with GEOS-4. The very large changes in the effects on MCF and CH_4 lifetimes due to the RAN and LIN assumptions (i.e., -6% vs. -11%) are due to the large changes in the effects on OH concentrations, as discussed above. The relatively longer lifetimes of MCF and CH_4 , even in clear-sky conditions, reflect lower OH concentrations, especially in the tropical lower troposphere, than those in the simulations with GEOS1-STRAT and GEOS-3. However, sorting out the factors responsible for these OH differences is difficult and is beyond the scope of this study.

5.2. Zonal Mean

Figure 5 shows simulated percentage changes in monthly zonal mean OH and O_3 due to the radiative effects of clouds for June when the model is driven by GEOS1-STRAT, GEOS-3 and GEOS-4, respectively. As with photolysis frequencies (**Figure 4**), the regions of OH enhancements and reductions due to the radiative impact of clouds show similar patterns with

GEOS1-STRAT and GEOS-3 because of similar vertical distributions of clouds in the two archives, although the magnitude of their respective relative changes in OH are different. In the tropics, OH is enhanced by up to ~5% (GEOS1-STRAT) or ~5-10% (GEOS-3) above the deep convective clouds, and reduced by ~5-10% (GEOS1-STRAT) or ~5-20% (GEOS-3) below, reflecting the backscattering (attenuation) of solar radiation above (below) the clouds. At NH midlatitudes, OH is enhanced by ~2-5% (GEOS1-STRAT) or ~5-10% (GEOS-3) above the low-level clouds; at SH subtropics, OH is enhanced by ~5%; at SH high latitudes, the impact of clouds on OH does not show consistent patterns. Near the surface, OH decreases by up to ~15-35% because of clouds, with the largest percentage decreases occurring at midlatitudes. By contrast, with GEOS-4, OH is enhanced (by ~5-10%) in most of the troposphere and is reduced (by up to ~20%) only near the surface (<~1km). Again, enhanced OH in the tropical middle troposphere is a result of the optically much thinner clouds in the tropical upper troposphere in GEOS-4, allowing solar UV radiation to not only penetrate down but be reflected back by low-level clouds.

With GEOS1-STRAT and GEOS-3, the maximum impact of clouds on O₃ (~2-5%) is seen in the tropical upper troposphere with a trivial impact elsewhere (**Figure 5**, right panels). The pattern of enhancements above clouds and reductions below clouds for OH are not seen for O₃, partly reflecting the relatively long lifetime of O₃ and the short lifetime of OH. More importantly, the tropical lower troposphere is overall a regime of net O₃ loss (~1 ppbv/day on zonal average) due to a low NO_x environment; therefore, the radiative effects of tropical deep convective clouds suppress this net O₃ loss (e.g., by a few percent with GEOS-3) primarily via the reaction $O(^1D) + H_2O \rightarrow 2 OH$, increasing O₃ in this part of the troposphere. On the other hand, with GEOS-4, the overall impact of clouds on O₃ is small, with a maximum in the middle/upper troposphere at NH high latitudes. We showed in *Liu et al.* [2006] that tropical upper tropospheric O₃ is much less sensitive to the radiative effects of clouds in the GEOS-Chem model (driven with GEOS-3) than previously reported by *Tie et al.* [2003] using the MOZART-2 model (~5% versus ~20-30%). Here we find that when driven with the other two meteorological archives that feature either different magnitudes of column CODs or different vertical distributions in the vertical, GEOS-Chem still shows much less sensitivity of tropospheric O₃ to the radiative effects of clouds than does MOZART-2. Indeed, our result was quite comparable to that of *Wild* [2007] who found a global O₃ burden change of 2.5% when all cloud cover was removed in the FRSGC/UCI CTM. It appears, however, that the global distributions of clouds in the MOZART-2 model used by *Tie et al.* [2003] are similar to those in GEOS-4, both underestimating the optical depth due to high clouds in the tropics. These suggest that differing cloud fields including cloud vertical distributions cannot explain the majority of the discrepancies between the results from GEOS-Chem and MOZART-2. A ~20-30% increase in tropical upper tropospheric O₃ solely due to the radiative effects of clouds is too large, as we previously argued [*Liu et al.*, 2006].

6. Sensitivity to the Magnitude of Cloud Optical Depths

Comparing the effects of clouds in GEOS1-STRAT and GEOS-3, which feature similar vertical distribution of clouds, provides a sense of the sensitivity of simulated photolysis frequencies and tropospheric oxidants to the magnitude of CODs. To see the full range of sensitivity to COD magnitude, we examine in this section sensitivity simulations where the magnitude of 3-D CODs is progressively adjusted. We choose GEOS-3 (versus GEOS-4) for these perturbation experiments because its high clouds are optically thicker and probably more

realistic (section 3). These results should prove useful for understanding the radiative impact of clouds in other models with similar vertical distributions of clouds. They will also help understand how potential changes in the magnitude of CODs in a future climate may affect tropospheric chemistry. To help understand the results from our sensitivity simulations for different seasons, we first examine the seasonal and latitudinal variability in the distributions of clouds and their effects on photolysis frequencies and tropospheric oxidants.

Figure 6 shows the zonal mean latitude-height cross-sections of GEOS-3 monthly mean cloud extinction coefficient (km^{-1}) for January, March, June and October. Vertical profiles of monthly zonal mean cloud extinction coefficients at selected latitudes (46°N , 38°N , 30°N , equator, 30°S , 38°S , and 46°S) are shown in **Figure 7** (0-16km) and **Figure 8** (0-3km), respectively. In all months, GEOS-3 shows high clouds associated with deep convection in the tropics and low-level stratiform clouds at middle and high latitudes. While the overall patterns of cloud distributions are similar in different months, there are significant regional differences. In the tropics, extinction coefficients have a local maximum in the upper troposphere in Jan, March and June; they are more uniform in the upper and middle troposphere in October. In the middle/high latitudes, the SH exhibits substantially larger extinction in the lower troposphere than the NH does (**Figure 8**). These relative distributions of clouds will affect how photolysis frequencies and tropospheric oxidants respond to the varying magnitude of CODs.

We show in **Figure 9** the model calculated percentage changes in monthly zonal mean photolysis frequencies $J(\text{O}^1\text{D})$ because of the radiative effects of clouds indicated in **Figures 7 and 8**. In the tropics, $J(\text{O}^1\text{D})$ are enhanced above and reduced below about 7km (5km) in January, March and June (October). In January, March and June, the local maximum in cloud extinction coefficients in the upper troposphere prevents solar UV radiation from penetrating down, leading to reductions in $J(\text{O}^1\text{D})$ in more of the troposphere; this is particularly true for June. In October, the cloud extinction coefficients in the middle and upper troposphere are more uniformly distributed and the reflection from lower levels becomes more important, resulting in reductions in $J(\text{O}^1\text{D})$ in less of the troposphere. In the SH, $J(\text{O}^1\text{D})$ is enhanced in most of the troposphere except near the surface where it is reduced by $\sim 10\text{-}30\%$. In the NH, by contrast, this transition from enhancement to reduction occurs at higher altitudes ($\sim 2\text{-}6\text{km}$) in all seasons except June, reflecting higher and optically thicker clouds in the NH than in the SH during those seasons (**Figure 7**). In June, the NH exhibits decreased cloud extinction in the lower free troposphere ($\sim 1\text{-}2\text{ km}$, **Figures 6 and 8**), allowing more solar radiation reflected back by boundary layer thick clouds. The impact of clouds on $J(\text{NO}_2)$ (not shown) is similar to that on $J(\text{O}^1\text{D})$, but as discussed earlier, $J(\text{NO}_2)$ is more sensitive to the presence of clouds than $J(\text{O}^1\text{D})$. The impact of clouds on OH concentrations at different latitudes and seasons (not shown) are similar to those on $J(\text{O}^1\text{D})$ and $J(\text{NO}_2)$.

Figure 10 shows the model sensitivities of regional and global mean OH to the magnitude of CODs in January, March, June and October. $J(\text{O}^1\text{D})$ and $J(\text{NO}_2)$ show similar sensitivities (not shown). Plotted are the percentage changes in global and column (at selected latitudes as indicated in **Figures 7-9**) mean OH relative to the standard simulation as the magnitudes of 3-D CODs are adjusted progressively from -100% to 100% . A -50% change in CODs corresponds to half of the original GEOS-3 CODs with the same 3-D spatial distributions. Global mean OH (solid line) is shown to have only modest changes at all CODs. Again, this reflects the opposite effects of enhanced (weakened) photochemistry above (below) clouds. It also reflects the overall opposite effects of clouds in the NH and the SH. The slopes of the global mean curve indicate that global mean OH shows the strongest sensitivity to CODs at the low end. The slopes remain

positive and decrease with increasing CODs during January and October; in contrast, the slopes change from positive to negative with increasing CODs during March and June. The decreasing slopes with increasing CODs reflect saturation at large CODs.

In January, March and October, the higher and optically thicker clouds in the NH (**Figures 6-8**) lead to a decreasing trend in OH as the CODs increase (**Figure 10**); the thinner clouds in the SH middle troposphere (**Figures 6-8**) allow solar radiation to be reflected by the low stratus clouds, resulting in an increasing trend in OH as the CODs increase (**Figure 10**). In June, OH is less sensitive to CODs than in other months ($\pm 4\%$ versus $\pm 15\%$) in both hemispheres. This reduced sensitivity is because boundary-layer clouds in GEOS-3 become optically thicker and mid-level clouds thinner in the NH while mid-level clouds become thicker at the SH mid-latitudes (**Figures 7-8**). The latter reflects enhanced frequency of mid-latitude cyclogenesis in the wintertime. Column mean OH concentrations at all latitudes show higher (lower) sensitivity at small (large) CODs.

We conclude that the modest effects of the perturbation to GEOS-3 CODs on global mean OH are due to the compensation between above-cloud enhancements and below-cloud reductions (in the vertical) and the opposite responses to this perturbation in the two hemispheres (in the horizontal). The effects would be larger if GEOS-4 cloud distributions were used in these perturbation experiments because of smaller compensations above and below clouds. Monotonic increases in global mean OH for January and October reflect the dominant backscattering from low-level clouds, while non-monotonic changes for March and June are a result of the sufficiently large optical depths due to high clouds which allow less solar radiation to penetrate down to the lower levels and thus limit backscattering from low-level clouds. On the other hand, global and regional column mean O_3 essentially increase monotonically when the CODs are varied from -100% to 100%, but the effects of clouds remain modest ($<5\%$) (not shown).

7. Sensitivity to Cloud Absorption of Solar Radiation

We present in this section a cautionary note that 0.99 is too low a value for cloud single scattering albedo (SSA) and is not consistent with current knowledge of cloud absorption of solar radiation at the ultraviolet wavelengths relevant to tropospheric chemistry. This unrealistic value was cited in some recent literature of tropospheric chemistry. Pure water clouds are inefficient absorbers and their SSAs are between 0.999990 and 0.999999 in the ultraviolet wavelength range [*Hu and Stamnes, 1993*]. Even for contaminated clouds containing black carbon, SSA is still between 0.999 and 0.9999 at 550nm [*Chylek et al., 1996*]. Using a SSA value as low as 0.99 would lead to large reductions in below-cloud actinic fluxes and thus photolysis frequencies and to a lesser extent above the clouds.

We show in **Figure 11** the simulated percentage changes in the June monthly zonal mean $J(O^1D)$, $J(NO_2)$ and OH due to the radiative effects of clouds (GEOS-3), using cloud SSA=0.99 (left panels) and SSA=0.999 (right panels), respectively. These plots can be compared to those presented earlier in this paper (**Figure 4 and 5**) where SSA=1.0 was used in the standard cloudy-sky simulation. Using SSA=0.99 is seen to significantly decrease the calculated radiative effects of clouds, both below and above the clouds. We find that while a 1 per mil decrease in SSA (from 1.0 to 0.999) leads to only ~ 1 -2% decrease in $J(O^1D)$, $J(NO_2)$ and OH concentrations, 1% decrease in SSA (from 1.0 to 0.99) would decrease photolysis frequencies and OH by ~ 5 -10% in most of the troposphere. This reflects the strong sensitivity of cloud transmittance and cloud albedo to cloud absorption. Similar calculations with GEOS-4 indicate smaller effects, suggesting in this case the magnitude of CODs is more important than the vertical distribution. In

a word, caution should be exercised not to use for cloud SSA a value lower than 0.999 (e.g., 0.99) in model simulations of tropospheric chemistry.

8. Summary and Conclusions

We have examined the sensitivity of photolysis frequencies and key tropospheric oxidants to cloud vertical distributions and optical properties in a global 3-D CTM (GEOS-Chem) coupled with the Fast-J radiative transfer algorithm. The model was driven with a series of meteorological archives (GEOS1-STRAT, GEOS-3 and GEOS-4) generated by the GEOS DAS at the NASA GMAO, which have significantly different cloud optical depths (CODs) and vertical distributions. An approximate random overlap (RAN) scheme was used to take into account the vertical subgrid variability of cloudiness (cloud overlap). The direct radiative effect of clouds on the tropospheric chemistry of the model was represented by subtraction of a simulation with zero CODs for photolysis calculations from a standard (cloudy-sky) simulation. Our objective was to improve our understanding of the role that different cloud fields played in the variability of tropospheric oxidants among global models in terms of the direct radiative effects of clouds on tropospheric chemistry.

We intercompared the GEOS effective column CODs under the RAN scheme and evaluated them with the satellite retrieval products of radiative mean CODs from the Moderate Resolution Imaging Spectroradiometer (MODIS) and the International Satellite Cloud Climatology Project (ISCCP). All CODs show peaks in the tropics associated with deep convective clouds and at midlatitudes associated with extratropical cyclones in the Northern Hemisphere (NH) and marine stratiform clouds in the Southern Hemisphere (SH). However, CODs differ substantially among the GEOS archives. In the tropics, GEOS-4 effective CODs are most close to MODIS and ISCCP radiative mean CODs; at mid-latitudes, GEOS-4 and GEOS-3 effective CODs appear to bracket MODIS and ISCCP radiative mean CODs. With respect to vertical distribution, clouds in GEOS-4 are optically much thinner in the tropical upper troposphere compared to those in GEOS1-STRAT and GEOS-3.

By examining the sensitivity of photolysis frequencies and tropospheric oxidants, with a focus on $J(\text{O}^1\text{D})$, $J(\text{NO}_2)$, OH and O_3 , to the three GEOS cloud fields, we illustrated that the direct radiative impact of clouds on global tropospheric chemistry is more sensitive to cloud vertical distribution than to the magnitude of column COD. Specifically, our model calculations indicate that the changes in global mean OH ($J(\text{O}^1\text{D})$, $J(\text{NO}_2)$) due to the radiative effects of clouds in June are about 0.0% (0.4%, 0.9%), 0.8% (1.7%, 3.1%), and 7.3% (4.1%, 6.0%), for GEOS1-STRAT, GEOS-3 and GEOS-4, respectively. It is important to note that the distribution of photolysis frequencies and OH concentrations shows much larger changes than global mean values do. For instance, maximum decreases in OH concentrations of ~15-35% occur near the midlatitude surface. The effects on global mean OH are similar for GEOS1-STRAT and GEOS-3 due to their similar vertical distributions of clouds, even though the column CODs in the two archives differ by a factor of about 5. Despite a factor of 2 smaller optical depths than those clouds in GEOS-3, clouds in GEOS-4 have a much larger impact on global mean photolysis frequencies and OH. The reason is that with GEOS-4, more solar UV radiation is able to penetrate through the optically thin clouds in the upper troposphere, increasing backscattering from low-level clouds and leading to enhanced photochemical activity through most of the free troposphere. The net effects of clouds in the middle troposphere are largely determined by the competition between the radiative effects of high and low clouds.

With each of the three (GEOS1-STRAT, GEOS-3, and GEOS-4) cloud distributions, the model global burden of O₃ changes by only a few percent (<5%) as a result of radiative perturbations from clouds, consistent with the result of *Wild* [2007]. In all cases, tropical upper tropospheric O₃ is much less sensitive to the radiative effects of clouds than previously reported by *Tie et al.* [2003] who used the MOZART-2 model (~5% versus ~20-30%). We argue that differing cloud vertical distributions and optical depths, if present, cannot explain the majority of the discrepancies between the GEOS-Chem and MOZART models.

We performed model perturbation experiments to see the full range of the sensitivities of photolysis frequencies and tropospheric oxidants to CODs with varying magnitudes. The model driven by GEOS-3 predicts only modest changes in global mean OH concentrations when the magnitudes of 3-D CODs are progressively varied by -100% to 100% without altering cloud spatial distributions. It reflects the compensating effect between above-cloud enhancements and below-cloud reductions as well as the overall opposite responses to the cloud perturbation in the NH and the SH. The latter was because in most of the year the NH has clouds that are higher and optically thicker while the SH has thinner (thicker) clouds in the middle (lower) troposphere. Global mean OH shows the strongest sensitivity for small CODs and becomes more or less saturated for large CODs. On the other hand, the effects of clouds on global burden of O₃ in these perturbation experiments remain modest (<5%).

Caution should be exercised not to use a value for cloud single scattering albedo (SSA) lower than 0.999 in order to be consistent with the current knowledge of cloud absorption at the ultraviolet wavelengths relevant to tropospheric photochemistry. Realistic values for cloud SSA are between 0.999 and 1.0. Moreover, the calculated radiative effects of clouds are very sensitive to the specified cloud SSA. Using 0.99 for cloud SSA in our model driven by GEOS-3 would decrease simulated J(O¹D), J(NO₂), and OH concentrations by ~5-10% in most of the troposphere, relative to SSA=1.0.

Results from our sensitivity studies are robust with respect to varying cloud distributions and optical depths and have important implications for model intercomparisons and for climate feedback on tropospheric photochemistry. First, cloud vertical distributions and optical depths often vary from model to model and may contribute substantially to the model-model discrepancies in tropospheric OH (oxidation capability). While the differing magnitudes of column CODs may explain part of this discrepancy, the differing vertical distribution of clouds plays a more important role. Thus the impact of errors in the magnitude of CODs on simulated OH concentrations is smaller than that of errors in the vertical distribution of clouds of similar magnitude. Second, properly representing the vertical distribution of clouds in climate models and its response to climate change is more important for predicting the feedback of cloud changes in a warmer climate on tropospheric photochemistry. This requires an improved representation of clouds, especially their vertical distribution, in current climate models. It is made possible by the launchings of CloudSat and CALIPSO satellites (April 2006) where a unique dataset of not only cloud optical and physical properties but also their vertical distributions will be available for evaluating and constraining the models.

Acknowledgments. This work was supported by NASA Langley Research Center. Thanks are due to Jennifer Logan (Harvard University) for discussions that inspired part of this work, Bernhard Mayer (Institute of Atmospheric Physics of DLR, Germany) for discussions regarding the cloud single scattering albedo, Yan Feng (University of California at San Diego) for communications about the effect of cloud overlap on photolysis frequencies, and Mat Evans

(University of Leeds, UK) for his comments on an earlier manuscript. MODIS and ISCCP products are distributed by NASA Goddard Level 1 and Atmosphere Archive and Distribution System (<http://ladsweb.nascom.nasa.gov>) and Langley Atmospheric Sciences Data Center, respectively. The GEOS-Chem model is managed by the Atmospheric Chemistry Modeling Group at Harvard University with support from the NASA Atmospheric Chemistry Modeling and Analysis Program (ACMAP). The views, opinions, and findings contained in this report are those of the authors and should not be construed as an official NASA, NOAA or U.S. government position, policy, or decision.

Appendix. Derivation of MODIS and ISCCP all-sky grid-box cloud optical depths

The albedo (R_c) of a non-absorbing, horizontally homogeneous cloud is given by the two-stream approximation [*Lacis and Hansen, 1974; Seinfeld and Pandis, 1998*] as

$$R_c = \frac{\sqrt{3}(1-g)\tau_c}{2 + \sqrt{3}(1-g)\tau_c} \quad (\text{A1})$$

where τ_c is in-cloud optical depth (COD) and g is the asymmetry factor. Assuming the value of g for cloud drops of radius much greater than the wavelength of visible light is 0.85, the above equation becomes

$$R_c = \frac{\tau_c}{\tau_c + 7.7} \quad (\text{A2})$$

Therefore, with the average cloud albedo preserved, MODIS or ISCCP grid-box mean cloud albedo (R_c') can be expressed as

$$R_c' = \frac{\tau_c'}{\tau_c' + 7.7} = f \cdot \frac{\tau_c}{\tau_c + 7.7} \quad (\text{A3})$$

where τ_c' is *all-sky* grid-box radiative mean COD and f grid-box cloud fraction. Solving (4) for τ_c' , we have

$$\tau_c' = \frac{f\tau_c \cdot 7.7}{(1-f)\tau_c + 7.7} \quad (\text{A4})$$

where the unprimed τ_c is the in-cloud radiative mean COD (the proxy geometric mean COD in the case of MODIS) for the region and period under consideration.

References

- Bey I., D. J. Jacob, R. M. Yantosca, J. A. Logan, B. Field, A. M. Fiore, Q. Li, H. Liu, L. J. Mickley, and M. Schultz (2001), Global modeling of tropospheric chemistry with assimilated meteorology: Model description and evaluation, *J. Geophys. Res.*, *106*, 23,073-23,096.
- Bloom, S., A. da Silva, D. Dee, M. Bosilovich, J.-D. Chern, S. Pawson, S. Schubert, M. Sienkiewicz, I. Stajner, W.-W. Tan, and M.-L. Wu (2005). Documentation and Validation of the Goddard Earth Observing System (GEOS) Data Assimilation System - Version 4. *Technical Report Series on Global Modeling and Data Assimilation* (Editor Max J. Suarez), NASA/TM-2005-104606, Vol. 26, NASA Goddard Space Flight Center, Greenbelt, Maryland, April.
- Briegleb, B.P. (1992), Delta-Eddington approximation for solar radiation in the NCAR Community Climate Model, *J. Geophys. Res.*, *97*, 7603-7612.
- Chylek, P., et al. (1996), Black carbon and absorption of solar radiation by clouds, *J. Geophys. Res.*, *101*, 23,365-23,371.
- Crawford, J.H., D. Davis, G. Chen, R. Shetter, M. Muller, J. Barrick, and J. Olson (1999), An assessment of cloud effects on photolysis rates: Comparison of experimental and theoretical values, *J. Geophys. Res.*, *104*, 5725-5734.
- Evans, M.J., and D.J. Jacob (2005), Impact of new laboratory studies of N₂O₅ hydrolysis on global model budgets of tropospheric nitrogen oxides, ozone, and OH, *Geophys. Res. Lett.*, *32*, L09813, doi:10.1029/2005GL022469.
- Feng, Y., J.E. Penner, S. Sillman, and X. Liu (2004), Effects of cloud overlap in photochemical models, *J. Geophys. Res.*, *109*, D04310, doi:10.1029/2003JD004040.
- Heald, C.L., D.J. Jacob, R.J. Park, B. Alexander, T.D. Fairlie, D.A. Chu, and R.M. Yantosca (2006), Transpacific transport of Asian anthropogenic aerosols and its impact on surface air quality in the United States, *J. Geophys. Res.*, *111*, D14310, doi:10.1029/2005JD006847.
- Herman, J.R., and E.A. Celarier (1997), Earth surface reflectivity climatology at 340-380 nm from TOMS data, *J. Geophys. Res.*, *102*, 28,003-28,011.
- Hu, Y.X., and K. Stamnes (1993), An accurate parameterization of the radiative properties of water clouds suitable for use in climate models, *J. Climate*, *6*, 728-742.
- Intergovernmental Panel on Climate Change (IPCC) (2001), *Climate Change (2001): The Scientific Basis*, Cambridge University Press, UK.
- Intergovernmental Panel on Climate Change (IPCC) (2007), *Climate Change (2007): The Scientific Basis*, Cambridge University Press, UK.
- Kiehl, J.T., et al. (1998), The National Center for Atmospheric Research Community Climate Model: CCM3, *J. Climate*, *11*, 1131-1150.
- Krol, M.C., and M. van Weele (1997), Implications of variations in photodissociation rates for global tropospheric chemistry, *Atmos. Environ.*, *31*, 1257-1273.
- Lacis, A.A., and J.E. Hansen (1974), A parameterization of the absorption of solar radiation in the Earth's atmosphere, *J. Atmos. Sci.*, *31*, 118-133.
- Lefer, B.L., R.E. Shetter, S.R. Hall, J.H. Crawford, and J.R. Olson (2003), Impact of clouds and aerosols on photolysis frequencies and photochemistry during TRACE-P: 1. Analysis using radiative transfer and photochemical box models, *J. Geophys. Res.*, *108*(D21), 8821, doi:10.1029/2002JD003171.
- Liu, H., J.H. Crawford, R.B. Pierce, P. Norris, S.E. Platnick, G. Chen, J.A. Logan, R.M. Yantosca, M.J. Evans, C. Kittaka, Y. Feng, and X. Tie (2006), Radiative effect of clouds on

- tropospheric chemistry in a global three-dimensional chemical transport model, *J. Geophys. Res.*, *111*, doi:10.1029/2005JD006403.
- Madronich, S. (1987), Photodissociation in the atmosphere: 1. Actinic flux and the effect of ground reflections and clouds, *J. Geophys. Res.*, *92*, 9740–9752.
- Mao, H., W.-C. Wang, X.-Z., Liang, and R.W. Talbot (2003), Global and seasonal variations of O₃ and NO₂ photodissociation rate coefficients, *J. Geophys. Res.*, *108*(D7), 4216, doi:10.1029/2002JD002760.
- Martin, R.V., D.J. Jacob, J.A. Logan, I. Bey, R.M. Yantosca, A.C. Staudt, Q. Li, A.M. Fiore, B.N. Duncan, H. Liu, P. Ginoux, and V. Thouret (2002), Interpretation of TOMS observations of tropical tropospheric ozone with a global model and in-situ observations, *J. Geophys. Res.*, *107*, 4351, doi:10.1029/2001JD001480.
- Martin, R.V., C.E. Sioris, K. Chance, T.B. Ryerson, T.H. Bertram, P.J. Wooldridge, R.C. Cohen, J.A. Neuman, A. Swanson, and F.M. Flocke (2006), Evaluation of space-based constraints on global nitrogen oxide emissions with regional aircraft measurements over and downwind of eastern North America, *J. Geophys. Res.*, *111*, D15308, doi:10.1029/2005JD006680.
- McLinden, C.A., S.C. Olsen, B. Hannegan, O. Wild, M.J. Prather, and J. Sundet (2000), Stratospheric ozone in 3-D models: A simple chemistry and the cross-tropopause flux, *J. Geophys. Res.*, *105*, 14,653-14,665.
- Norris, P. M., and A. M. da Silva (2007), Assimilation of satellite cloud data into the GMAO Finite-Volume Data Assimilation System using a parameter estimation method. Part I: Motivation and algorithm description, *J. Atmos. Sci.*, *64*, 3880-3895.
- Oreopoulos, L., and R. F. Cahalan (2005), Cloud inhomogeneity from MODIS. *J. Climate*, *18*, 5110–5124.
- Park R. J., D. J. Jacob, B. D. Field, R. M. Yantosca, M. Chin (2004), Natural and transboundary pollution influences on sulfate-nitrate-ammonium aerosols in the United States: Implications for policy, *J. Geophys. Res.*, *109*, D15204, doi:10.1029/2003JD004473.
- Platnick, S., M.D. King, S.A. Ackerman, W.P. Menzel, B.A. Baum, J.C. Riedi, and R.A. Frey (2003), The MODIS cloud products: Algorithms and examples from Terra, *IEEE Transactions on Geoscience and Remote Sensing*, *41*(2), 459-473.
- Quante, M. (2004), The role of clouds in the climate system, *J. Phys. IV France*, *121*, 61-86.
- Rossow, W.B., and R.A. Schiffer (1999), Advances in understanding clouds from ISCCP. *Bull. Am. Meteorol. Soc.*, *80*, 2261-2287.
- Rossow, W.B., A.W. Walker, D.E. Beuschel, and M.D. Roiter (1996), *International Satellite Cloud Climatology Project (ISCCP) documentation of new cloud datasets*, Int. Counc. Of Sci. Unions, Paris, January.
- Rossow, W.B., C. Delo, and B. Cairns (2002), Implications of the observed mesoscale variations of clouds for the Earth's radiation budget, *J. Climate*, *15*, 557-585.
- Seinfeld, J.H., and S.N. Pandis (1998), *Atmospheric Chemistry and Physics: From Air Pollution to Climate Change*, 1173-1174, pp.1326, John Wiley & Sons, Inc., New York.
- Slingo, J.M. (1987), The development and verification of a cloud prediction scheme for the ECMWF model, *Quart. J. Roy. Meteor. Soc.*, *113*, 899-927.
- Stephens, G.L. (2005), Cloud feedbacks in the climate system: A critical review, *J. Climate*, *18*, 237-273.
- Takacs, L.L., A. Molod, and T. Wang (1994), Documentation of the Goddard Earth Observing System (GEOS) general circulation model – version 1, *NASA Tech. Memo.*, *TM-104606*, 1.

- Tang, Y., et al. (2003), Impacts of aerosols and clouds on photolysis frequencies and photochemistry during TRACE-P: 2. Three-dimensional study using a regional chemical transport model, *J. Geophys. Res.*, *108*, 8822, doi:10.1029/2002JD003100.
- Thompson, A.M. (1984), The effect of clouds on photolysis rates and ozone formation in the unpolluted troposphere, *J. Geophys. Res.*, *89*, 1341-1349.
- Thompson, A.M., and R.W. Stewart (1991), Effect of chemical kinetics uncertainties on calculated constituents in a tropospheric photochemical model, *J. Geophys. Res.*, *96*, 13,089-13,108.
- Thompson, A.M. (1992), The oxidizing capacity of the Earth's atmosphere – Probable past and future changes, *Science*, *256*, 1157-1165.
- Tie, X., S. Madronich, S. Walters, R. Zhang, P. Rasch, and W. Collins (2003), Effect of clouds on photolysis and oxidants in the troposphere, *J. Geophys. Res.*, *108*(D20), 4642, doi:10.1029/2003JD003659.
- Wild, O. (2007), Modelling the global tropospheric ozone budget: exploring the variability in current models, *Atmos. Chem. Phys.*, *7*, 2643-2660.
- Wild, O., X. Zhu, and M.J. Prather (2000), Fast-J: Accurate simulation of in- and below-cloud photolysis in tropospheric chemical models, *J. Atmos. Chem.*, *37*, 245-282.
- Wu, S., L.J. Mickley, D.J. Jacob, J.A. Logan, R.M. Yantosca, and D. Rind (2007), Why are there large differences between models in global budgets of tropospheric ozone? *J. Geophys. Res.*, *112*, D05302, doi:10.1029/2006JD007801.
- Yang, H., and H. Levy (2004), Sensitivity of photodissociation rate coefficients and O₃ photochemical tendencies to aerosols and clouds, *J. Geophys. Res.*, *109*(D24), D24301, doi: 10.1029/2004JD005032.
- Zhang, M.H., et al. (2005), Comparing clouds and their seasonal variations in 10 atmospheric general circulation models with satellite measurements, *J. Geophys. Res.*, *110*, D15S02, doi:10.1029/2004JD005021.

Table 1. Simulated Percentage Changes in the Global Mean Concentrations of Tropospheric Chemical Species, Photolysis Frequencies and Global Mean Lifetimes of Methylchloroform (MCF) and CH₄ Due to the Radiative Effects of Clouds with Different Cloud Overlap Assumptions (RAN and LIN) in June and January^a, Following Table 4 of *Tie et al.* [2003] and Table 2 of *Liu et al.* [2006].

Quantity ^b	GEOS1-STRAT (1996)		GEOS-3 (2001)		GEOS-4 (2001)	
	RAN	LIN	RAN	LIN	RAN	LIN
June						
OH	0.00	-0.73	0.80	2.05	7.26	12.63
O ₃ ^c	1.68	3.01	3.20	5.22	0.90	1.39
NO _x ^d	1.65	2.88	3.95	6.35	1.35	2.29
HO ₂	-1.25	-2.27	-1.62	-2.29	0.82	1.48
CH ₂ O	0.54	1.38	1.73	3.32	-0.65	-0.98
CO	-0.33	0.11	-0.06	-0.36	-4.50	-7.50
J(O ¹ D)	0.40	-0.06	1.73	3.25	4.08	7.32
J(NO ₂)	0.85	0.85	3.11	5.90	5.96	10.40
J(CH ₂ O)	0.72	0.70	2.70	5.18	4.93	8.73
January						
OH	0.98	0.91	2.95	5.16	7.66	13.37
O ₃ ^c	1.45	2.61	1.91	3.39	0.87	1.37
NO _x ^d	1.01	1.68	3.89	5.86	2.43	3.72
HO ₂	-0.62	-1.22	-0.71	-1.00	0.99	1.79
CH ₂ O	0.71	1.54	1.49	2.61	-0.57	-1.00
CO	0.07	0.61	-0.16	-0.37	-3.28	-5.59
J(O ¹ D)	1.43	1.62	4.00	6.58	4.89	8.59
J(NO ₂)	1.81	2.32	5.72	9.43	7.14	12.06
J(CH ₂ O)	1.66	2.14	5.10	8.52	6.03	10.33
T (MCF) ^e	1.00	2.77	0.78	0.53	-6.47	-10.91
	(6.22) ^f	(6.33)	(6.68)	(6.66)	(7.36)	(7.02)
T (CH ₄) ^e	1.11	2.97	1.01	0.90	-6.40	-10.80
	(10.50) ^f	(10.70)	(11.25)	(11.23)	(12.35)	(11.77)

^aThe radiative effects of clouds is represented by subtraction of the clear-sky (zero cloud optical depths) simulation from the cloudy-sky simulation.

^bGlobal mean concentrations are calculated by dividing the global total moles of a species by those of air. Global mean photolysis frequencies are volume-weighted values. Thermal tropopause is locally diagnosed using the World Meteorological Organization (WMO) definition of tropopause.

^cActually the extended odd oxygen family defined as $O_x = O_3 + NO_2 + 2 \times NO_3 +$ peroxyacylnitrates + $HNO_4 + 3 \times N_2O_5 + HNO_3$.

^d $NO_x \equiv NO + NO_2$.

^ePercentage changes in global annual mean lifetimes of MCF and CH_4 . The lifetimes are derived as the ratio of the total burden of atmospheric MCF or CH_4 to the tropospheric loss rate against oxidation by OH.

^fValues in the parentheses indicate global annual mean lifetimes (years) of MCF and CH_4 under cloudy conditions.

Figure Captions

Figure 1. (a). GEOS1-STRAT (1996), GEOS-3 (2001) and GEOS-4 (2001) monthly zonal mean effective column cloud optical depths as a function of latitude are compared to MODIS (MOD08_M3.005, level-3 monthly global product at $1^\circ \times 1^\circ$ resolution) and ISCCP (D2, 280 km equal-area grid) retrievals (all-sky radiative mean) for June 2001. The Approximate Random Overlap (RAN, equation 1) is used to calculate GEOS effective column cloud optical depths. (b). June 2001 GEOS zonal mean total cloud fractions as a function of latitude, compared to ISCCP retrievals (thin black line) and MODIS retrievals (thick black lines — the dashed line is the MOD35 diurnal-average cloud mask and the solid line is the MOD06 COD-retrieval cloud fraction). Zonal means are calculated for MODIS and ISCCP data if there are less than 10% missing values over the longitudes. See text for details.

Figure 2. Latitude-height cross-sections of monthly zonal mean cloud extinction coefficient (left panels) and cloud fraction (right panels) for June in GEOS1-STRAT (1996), GEOS-3 (2001), and GEOS-4 (2001), respectively. The Approximate Random Overlap (RAN) is used to obtain GEOS grid-box effective cloud optical depths (equation 1). See text for details.

Figure 3. The global distributions of GEOS1-STRAT (1996), GEOS-3 (2001), and GEOS-4 (2001) monthly mean column effective cloud optical depths (left panels) are compared to MODIS and ISCCP retrievals (radiative mean) for March 2001. Note the smaller color scale for GEOS1-STRAT. The Approximate Random Overlap (RAN, see equation 1) is used to calculate GEOS column effective cloud optical depths. MODIS and ISCCP all-sky grid-box mean cloud optical depths are averages over both cloudy and clear regions with nonlinear weights that preserve the average cloud albedo. Also shown are the probability distribution functions (PDF) of global monthly mean cloud optical depths in each dataset (right bottom panel). See text for details.

Figure 4. Percentage changes in monthly zonal mean $J(O^1D)$ in the troposphere due to the radiative effects of clouds in June, as simulated by the GEOS-Chem model driven with GEOS1-STRAT (1996), GEOS-3 (2001) and GEOS-4 (2001), respectively. Filled contour levels are -50, -30, -20, -10, -5, -2, 0, 2, 5, 10, 20%. Dotted contours indicate negative changes.

Figure 5. Same as Figure 4, but shown for OH and O_3 concentrations. Contour levels are -50, -30, -20, -10, -5, -2, 0, 2, 5, 10, 20%. Dotted contours indicate negative changes.

Figure 6. Zonal mean latitude-height cross-sections of GEOS-3 monthly mean cloud extinction coefficient (km^{-1}) for January, March, June and October 2001.

Figure 7. Same as Figure 6, but shown as vertical profiles of monthly zonal mean cloud extinction coefficients (km^{-1}) at selected latitudes (46°N , 38°N , 30°N , equator, 30°S , 38°S , and 46°S) for January, March, June and October 2001. Also shown are averages over all latitudes (solid lines). Vertical profiles between the surface and 3 km where cloud extinction coefficients may exceed 1.0 km^{-1} are shown in Figure 8.

Figure 8. Same as Figure 7, but for the altitudes of 0-3 km.

Figure 9. Same as Figure 7, but for percentage changes in monthly zonal mean $J(O^1D)$ due to the radiative effects of clouds.

Figure 10. Sensitivities of mean tropospheric OH concentrations to the magnitude of cloud optical depths in January, March, June and October, as simulated by the GEOS-Chem model driven with GEOS-3 (2001). Plotted in the figure are the percentage changes in global (solid lines) and column (at selected latitudes, dot and dashed lines) mean OH relative to the standard simulation as the magnitude of 3-D cloud optical depths is adjusted progressively from -100% to 100%. A -50% change in cloud optical depths corresponds to half of the original GEOS-3 cloud optical depth with the same 3-D spatial distributions.

Figure 11. Simulated percentage changes in monthly zonal mean $J(O^1D)$, $J(NO_2)$ and OH in the troposphere due to the radiative effects of clouds in June (GEOS-3, 2001), using cloud SSA=0.99 (left panels) and SSA=0.999 (right panels), respectively.

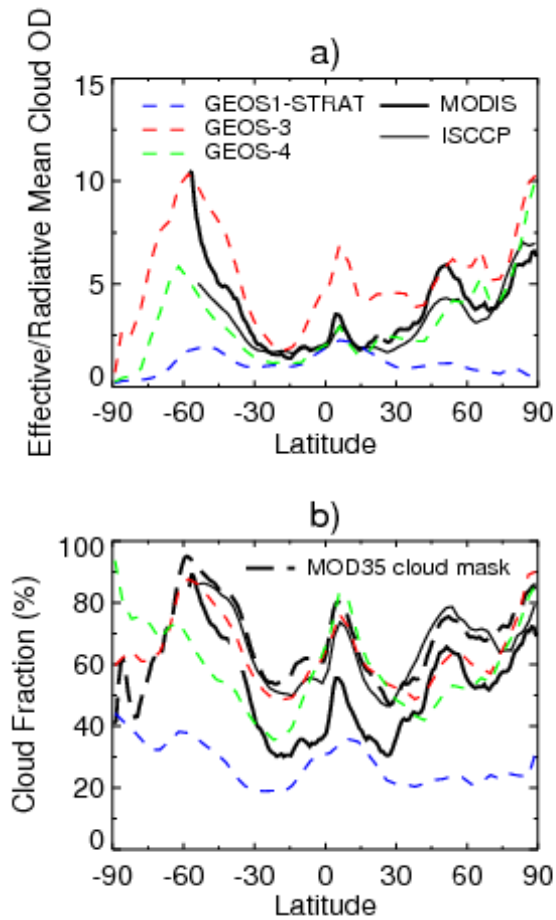


Figure 1. (a). GEOS1-STRAT (1996), GEOS-3 (2001) and GEOS-4 (2001) monthly zonal mean effective column cloud optical depths as a function of latitude are compared to MODIS (MOD08_M3.005, level-3 monthly global product at $1^\circ \times 1^\circ$ resolution) and ISCCP (D2, 280 km equal-area grid) retrievals (all-sky radiative mean) for June 2001. The Approximate Random Overlap (RAN, equation 1) is used to calculate GEOS effective column cloud optical depths. (b). June 2001 GEOS zonal mean total cloud fractions as a function of latitude, compared to ISCCP retrievals (thin black line) and MODIS retrievals (thick black lines — the dashed line is the MOD35 diurnal-average cloud mask and the solid line is the MOD06 COD-retrieval cloud fraction). Zonal means are calculated for MODIS and ISCCP data if there are less than 10% missing values over the longitudes. See text for details.

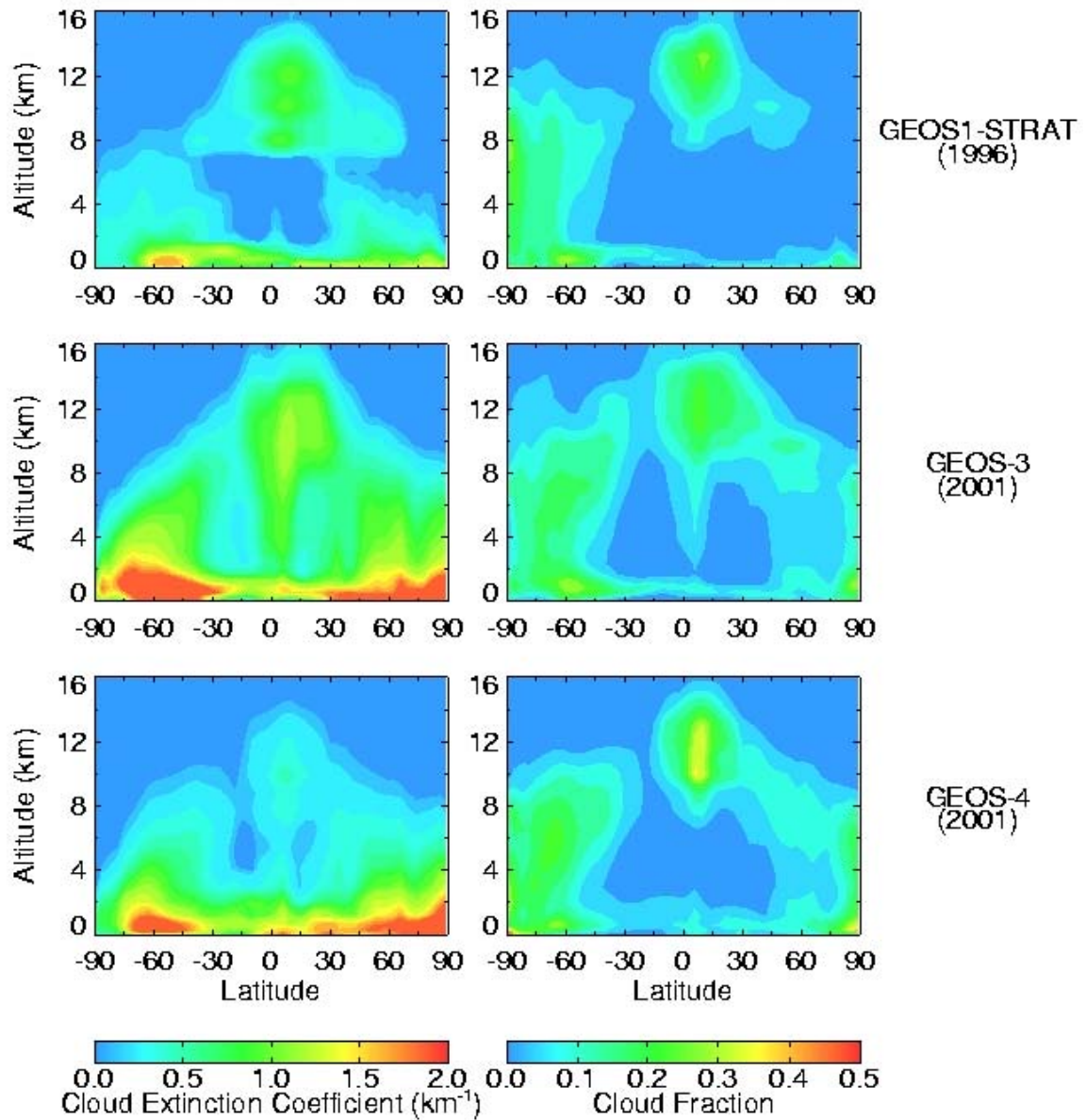


Figure 2. Latitude-height cross-sections of monthly zonal mean cloud extinction coefficient (left panels) and cloud fraction (right panels) for June in GEOS1-STRAT (1996), GEOS-3 (2001), and GEOS-4 (2001), respectively. The Approximate Random Overlap (RAN) is used to obtain GEOS grid-box effective cloud optical depths (equation 1). See text for details.

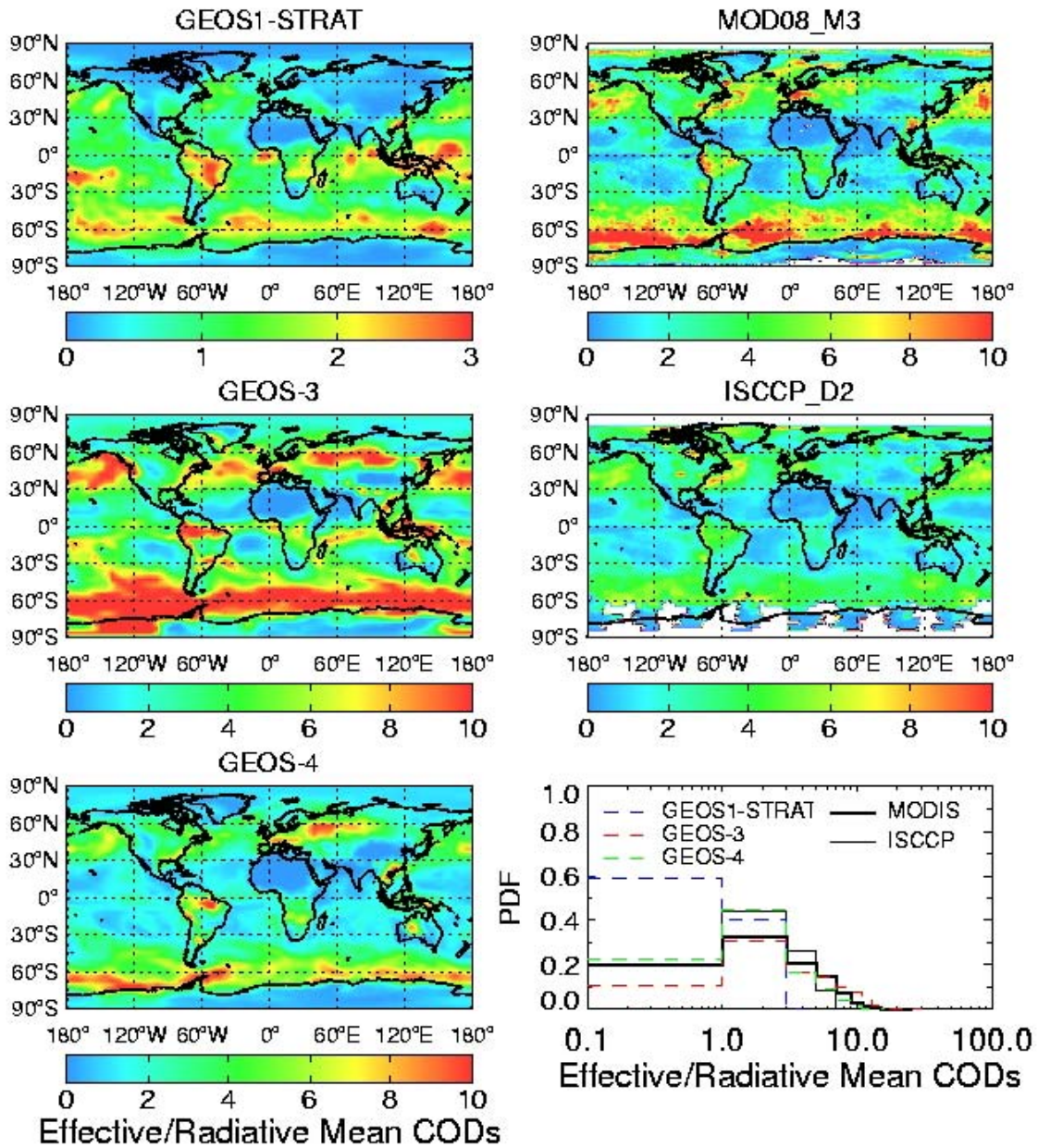


Figure 3. The global distributions of GEOS1-STRAT (1996), GEOS-3 (2001), and GEOS-4 (2001) monthly mean column effective cloud optical depths (left panels) are compared to MODIS and ISCCP retrievals (radiative mean) for March 2001. Note the smaller color scale for GEOS1-STRAT. The Approximate Random Overlap (RAN, see equation 1) is used to calculate GEOS column effective cloud optical depths. MODIS and ISCCP all-sky grid-box mean cloud optical depths are averages over both cloudy and clear regions with nonlinear weights that preserve the average cloud albedo. Also shown are the probability distribution functions (PDF) of global monthly mean cloud optical depths in each dataset (right bottom panel). See text for details.

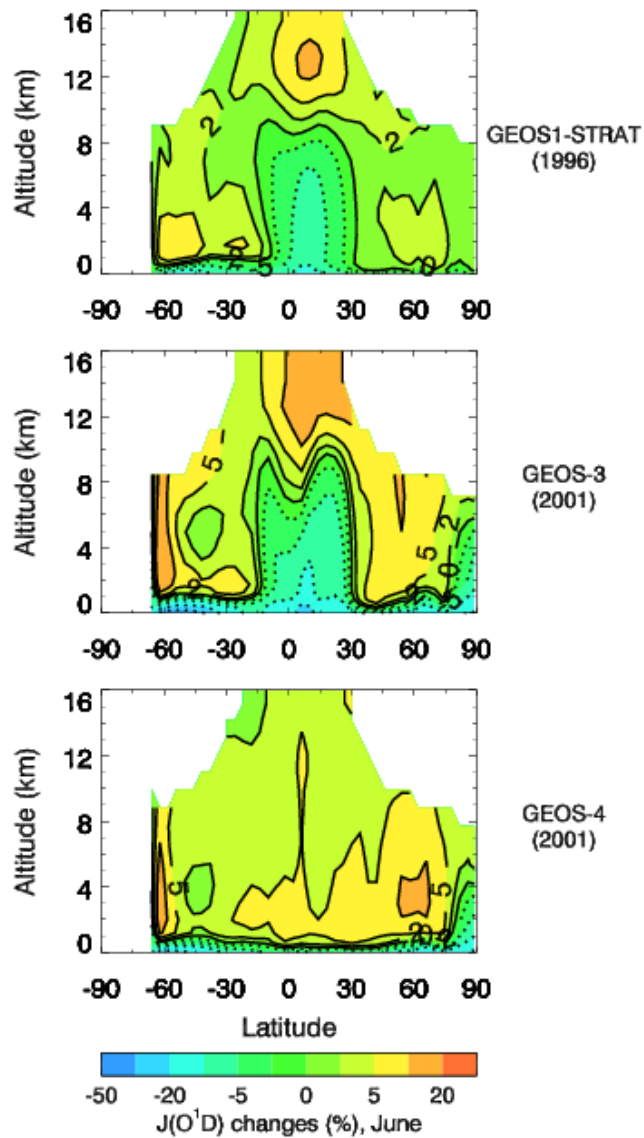


Figure 4. Percentage changes in monthly zonal mean $J(O^1D)$ in the troposphere due to the radiative effects of clouds in June, as simulated by the GEOS-Chem model driven with GEOS1-STRAT (1996), GEOS-3 (2001) and GEOS-4 (2001), respectively. Filled contour levels are -50, -30, -20, -10, -5, -2, 0, 2, 5, 10, 20%. Dotted contours indicate negative changes.

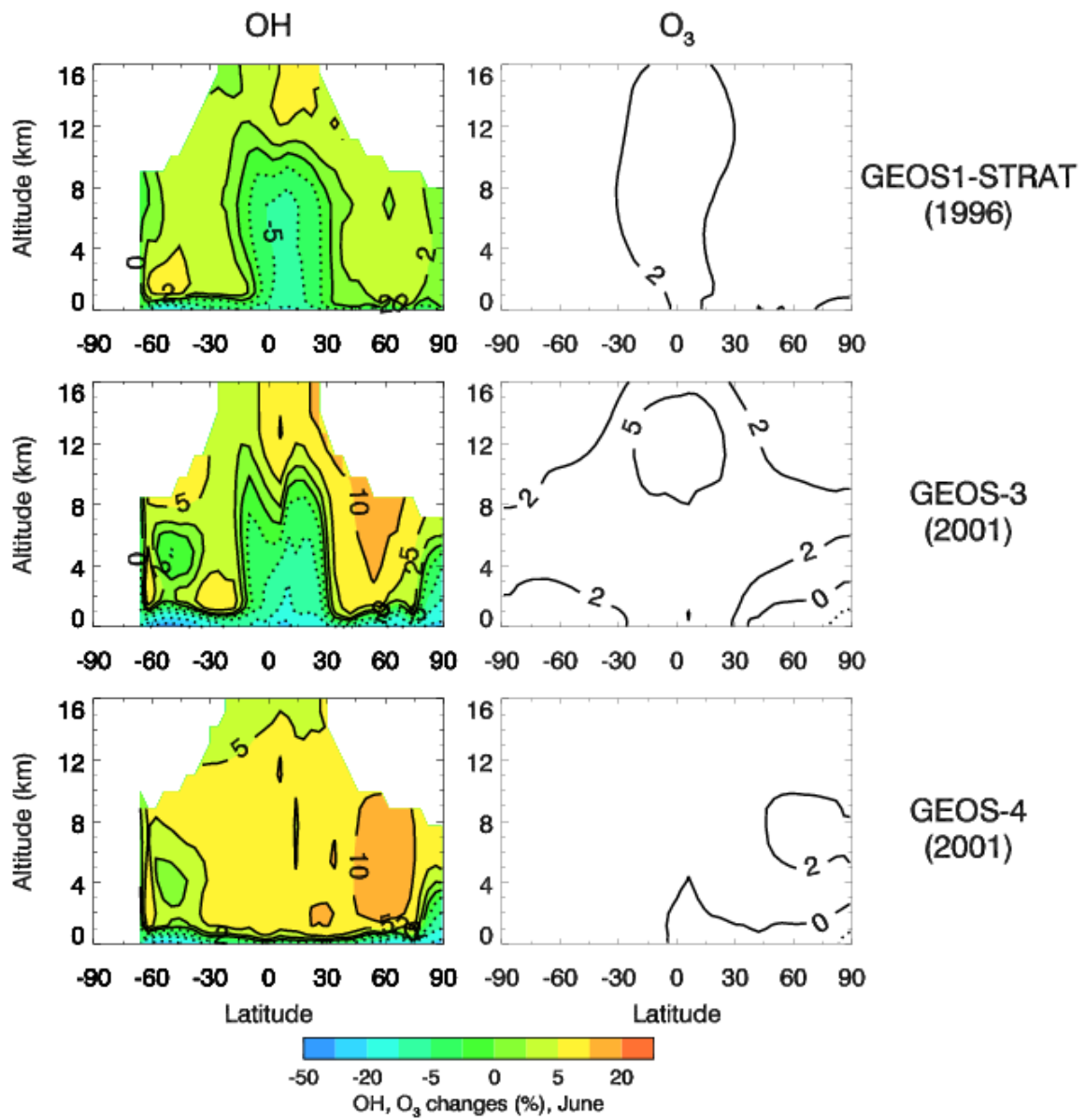


Figure 5. Same as Figure 4, but shown for OH and O₃ concentrations. Contour levels are -50, -30, -20, -10, -5, -2, 0, 2, 5, 10, 20%. Dotted contours indicate negative changes.

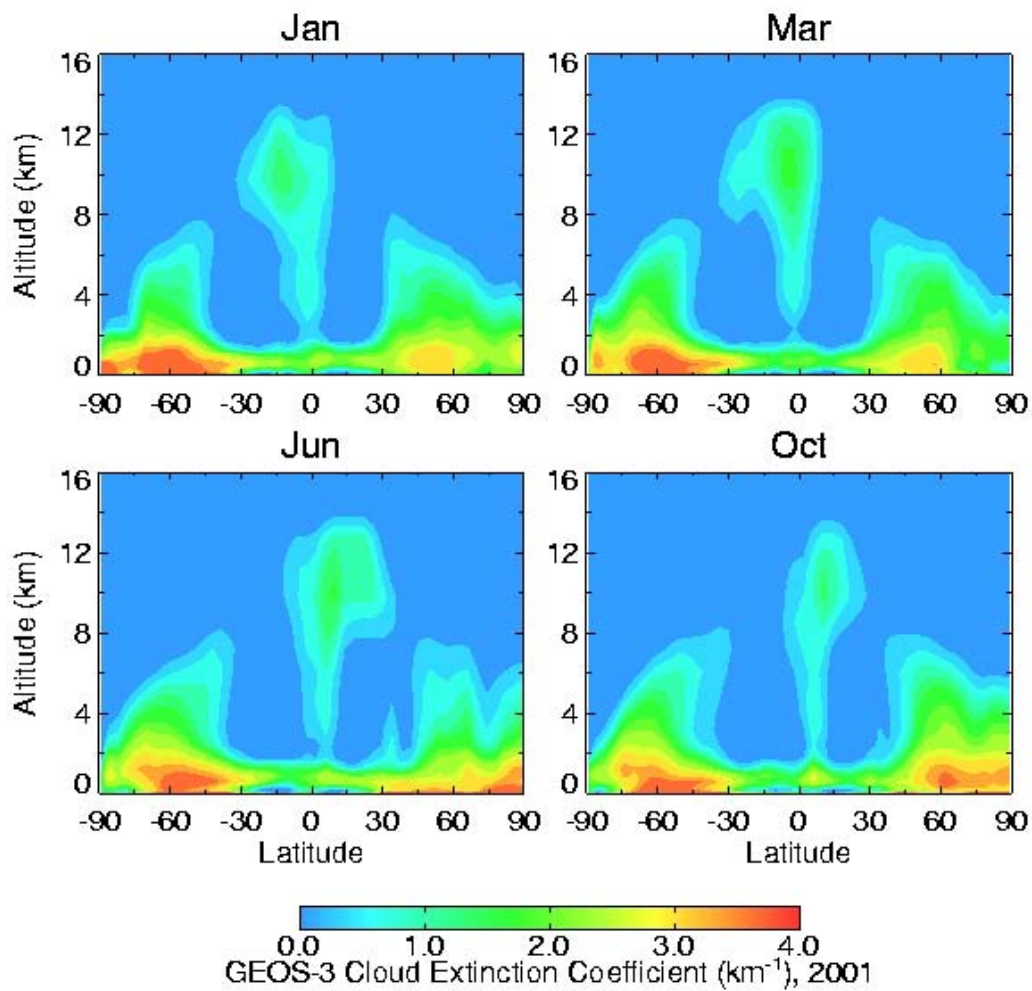


Figure 6. Zonal mean latitude-height cross-sections of GEOS-3 monthly mean cloud extinction coefficient (km^{-1}) for January, March, June and October 2001.

GEOS-3, 2001

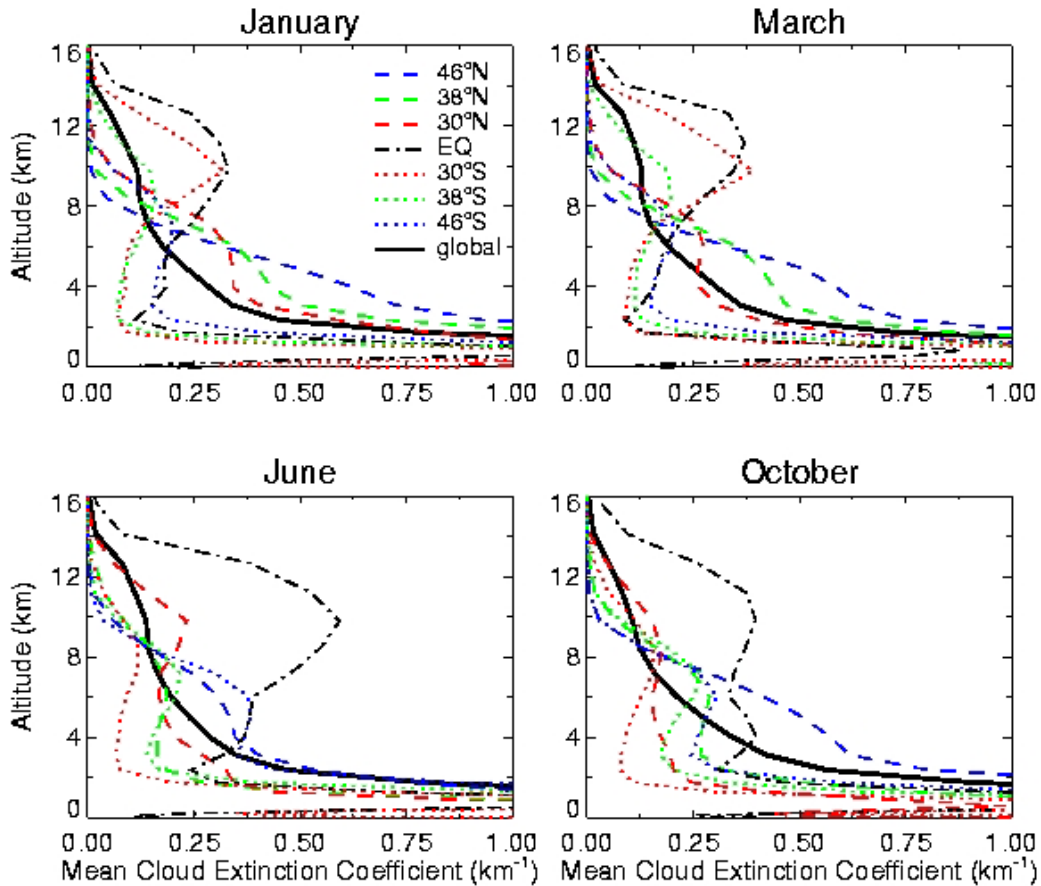


Figure 7. Same as Figure 6, but shown as vertical profiles of monthly zonal mean cloud extinction coefficients (km^{-1}) at selected latitudes (46°N , 38°N , 30°N , equator, 30°S , 38°S , and 46°S) for January, March, June and October 2001. Also shown are averages over all latitudes (solid lines). Vertical profiles between the surface and 3 km where cloud extinction coefficients may exceed 1.0 km^{-1} are shown in Figure 8.

GEOS-3, 2001

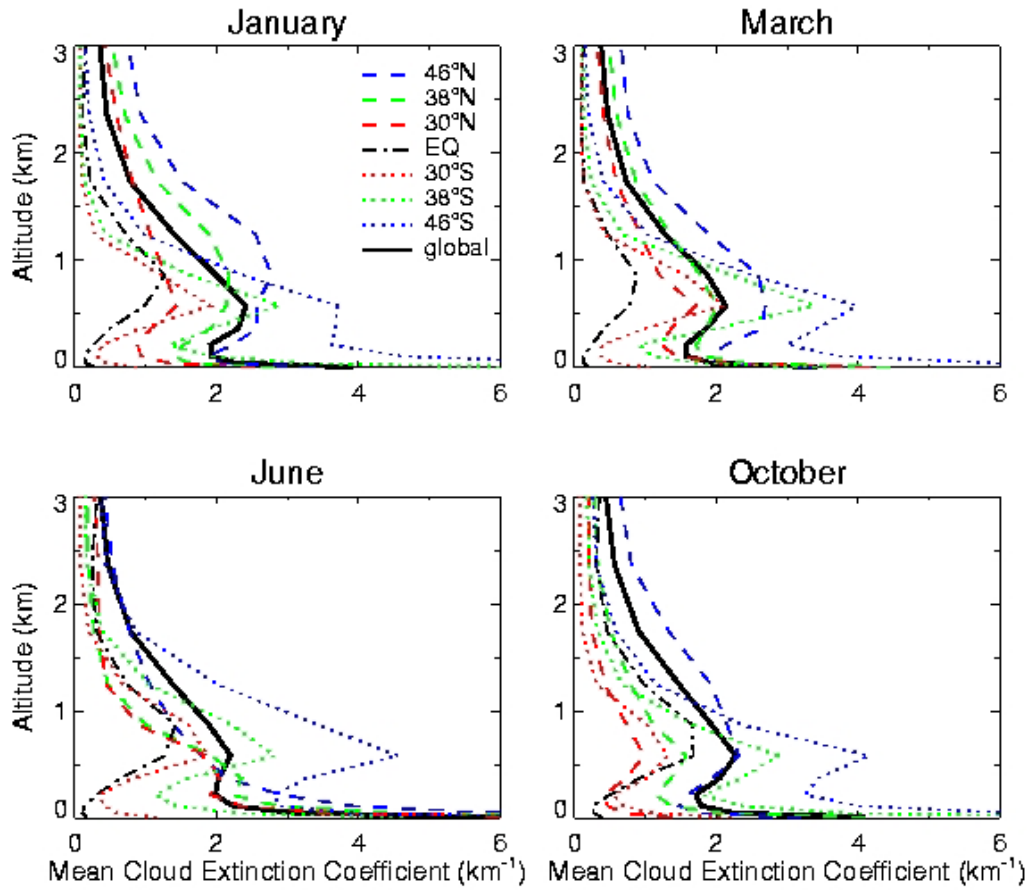


Figure 8. Same as Figure 7, but for the altitudes of 0-3 km.

GEOS-3, 2001

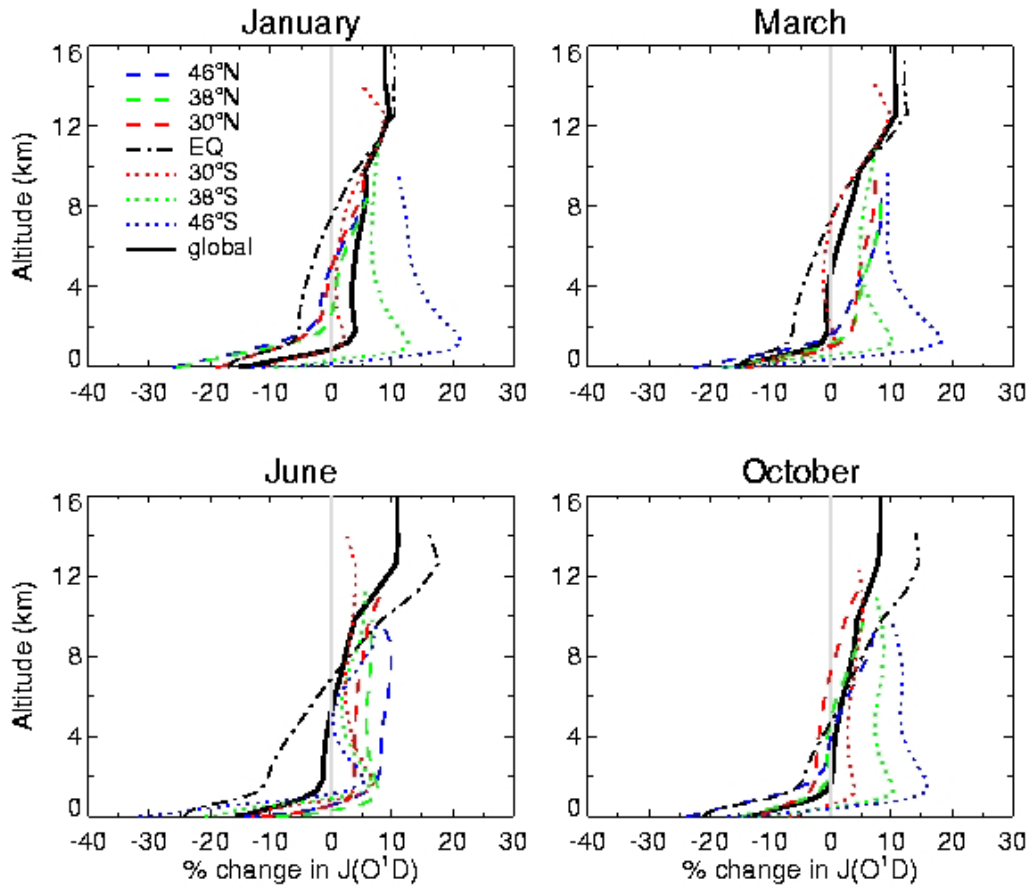


Figure 9. Same as Figure 7, but for percentage changes in monthly zonal mean $J(O^1D)$ due to the radiative effects of clouds.

RAN, GEOS-3, 2001

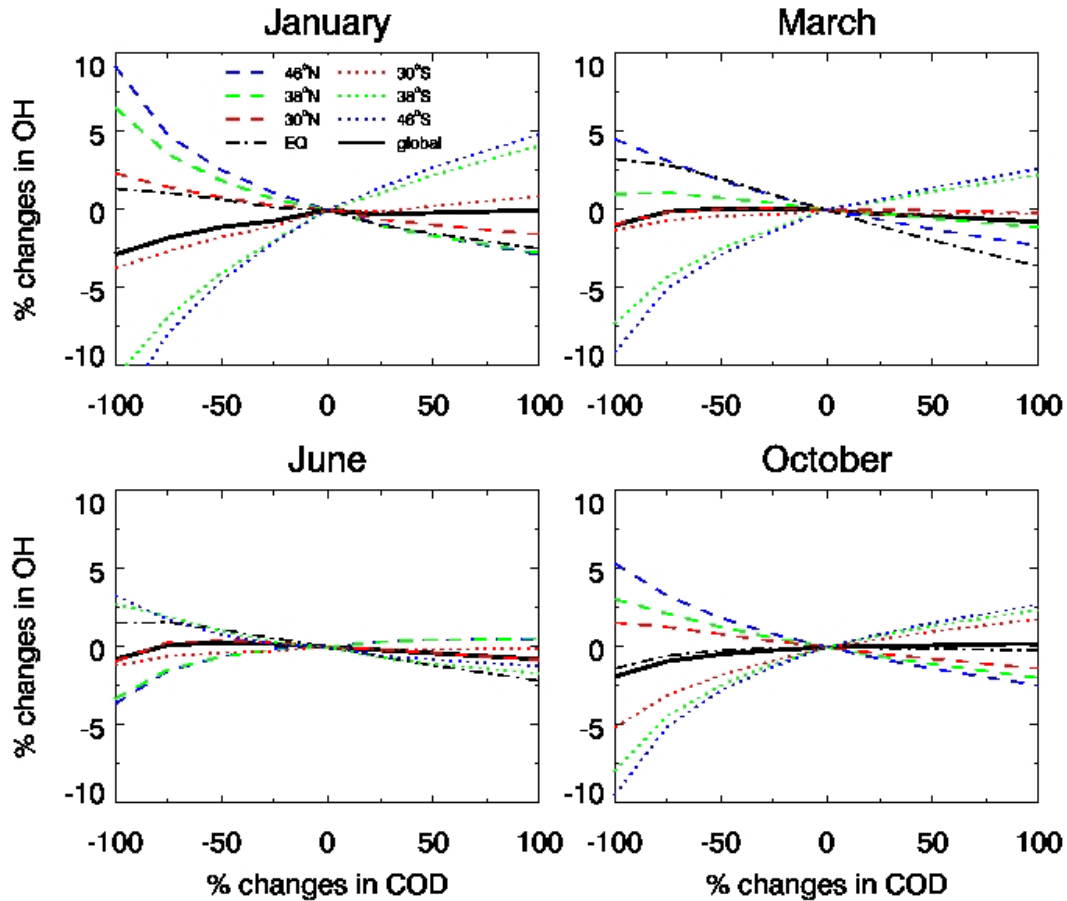


Figure 10. Sensitivities of mean tropospheric OH concentrations to the magnitude of cloud optical depths in January, March, June and October, as simulated by the GEOS-Chem model driven with GEOS-3 (2001). Plotted in the figure are the percentage changes in global (solid lines) and column (at selected latitudes, dot and dashed lines) mean OH relative to the standard simulation as the magnitude of 3-D cloud optical depths is adjusted progressively from -100% to 100%. A -50% change in cloud optical depths corresponds to half of the original GEOS-3 cloud optical depth with the same 3-D spatial distributions.

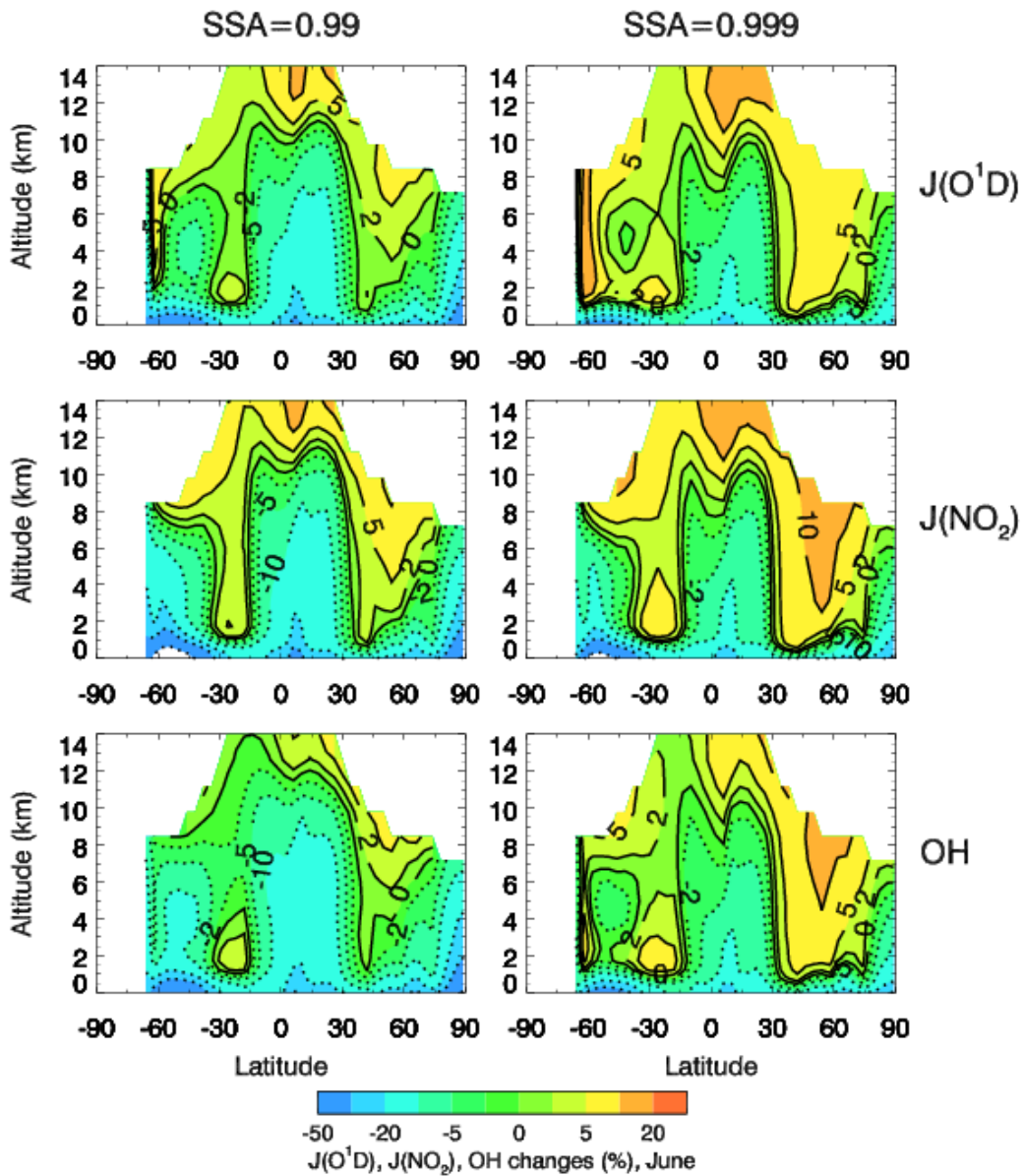


Figure 11. Simulated percentage changes in monthly zonal mean $J(O^1D)$, $J(NO_2)$ and OH in the troposphere due to the radiative effects of clouds in June (GEOS-3, 2001), using cloud SSA=0.99 (left panels) and SSA=0.999 (right panels), respectively.